

Copyright
by
Boonam Shin
2014

**The Thesis Committee for Boonam Shin
Certifies that this is the approved version of the following thesis:**

**Effects of Oversized Particles on the Dynamic Properties of Sand
Specimens Evaluated by Resonant Column Testing**

**APPROVED BY
SUPERVISING COMMITTEE:**

Kenneth H. Stokoe II, Supervisor

Robert B. Gilbert

**Effects of Oversized Particles on the Dynamic Properties of Sand
Specimens Evaluated by Resonant Column Testing**

by

Boonam Shin, B.E.

THESIS

Presented to the Faculty of the Graduate School of
The University of Texas at Austin
in Partial Fulfillment
of the Requirements
for the Degree of

MASTER OF SCIENCE IN ENGINEERING

The University of Texas at Austin

August, 2014

Acknowledgements

First and foremost, I would like to thank Dr. Stokoe for his guidance, support, and his unlimited enthusiasm. Your kindness and generosity will stand on my heart during the rest of my life. I have nothing but the highest respect for you and your devotion.

I am also very thankful to Dr. Gilbert not only for his review and comments pertaining to this thesis, but also for teaching the several finest geotechnical engineering course in this world. I would also like to acknowledge Dr. Rathge, Dr. Zomberg, Dr. El Mohtar and Dr. Wilson for their excellent courses of which I had the opportunity to participate in the geotechnical earthquake engineering world.

I would also like to extend my thanks to Bohyoung Lee, from whom I have learned and understood most of what I know in the Soil and Rock Dynamics Laboratory. I would like to thank Andrew Keene, Yaning Wang and Sungmoon Hwang, who helped me in the testing of these specimens and were more of a friend than a co-worker. I would also like to extend my appreciations to my sincere friends and colleagues Julia Robert, Jung Su Lee, Moo Yeon Kim, Alicia Zapata for all of the effort and help.

Lastly, I would like to thank my parents, my sisters, and all my friends for their constant prayers, advice, and friendship. Most of all, I would like to thank my lovely wife, Jieun Lee, for being my endless love and for carrying me all this time. I really would like to look forward to seeing my son soon. Lastly, I would like to thank our Lord and Savior Jesus Christ for being our strength and hope in all things.

Abstract

Effects of Oversized Particles on the Dynamic Properties of Sand Specimens Evaluated by Resonant Column Testing

Boonam Shin, M.S.E.

The University of Texas at Austin, 2014

Supervisor: Kenneth H. Stokoe II

This study was motivated by the fact that many times intact specimens with a number of oversized particles are dynamically tested in the laboratory and the impact of the particles on the dynamic properties is unknown. The effects of oversized particles represented by gravel particles on the shear modulus (G) and material damping ratio (D) of a uniform sand were evaluated in the linear ($\gamma \leq 0.001\%$) and nonlinear ($\gamma > 0.001\%$) ranges of shear strain with combined resonant column and torsional shear (RCTS) equipment. The sand used in this investigation is a uniform sand as a reference, well-characterized material on the dynamic properties. Sand-gravel specimens were constructed using the undercompaction method. A variety of rounded gravel particles was used in building the specimens. Dynamic tests on the sand-gravel specimens were performed, and the tests results are presented.

Among the findings of this investigation are that, compared to uniform sand: (1) oversized gravel particles symmetrically located along the longitudinal axis in uniform sand generally decreased slightly the small-strain shear modulus (G_{\max}), (2) oversized gravel particles asymmetrically located away from the longitudinal axis of rotation resulted in slight increases in G_{\max} and the small-strain material damping ratio (D_{\min}), (3) the $G - \log \gamma$ relationships of sand-gravel specimens with asymmetrically located gravel particles are generally above those with gravel particles symmetrically located along the longitudinal axis, and (4) the $G/G_{\max} - \log \gamma$ relationships of all specimens were reasonably close for the nonlinear ranges covered in these tests ($\gamma < 0.05\%$ and $G/G_{\max} > 0.6$).

As long as the oversized particles were near the axis of rotation, the particles had little effect on the dynamic properties (G_{\max} , D_{\min} and $G - \log \gamma$ relationships) regardless of sizes and numbers of particles. However, once the oversized particles were located away from the axis of rotation and closer to the perimeter of the specimen, the oversized particles influenced the dynamic properties. Finally, the additions of oversized particles located both symmetrically and asymmetrically in the uniform sand specimens have little impact on the nonlinear dynamic properties ($G/G_{\max} - \log \gamma$ and $D - \log \gamma$ relationships) which compared well with uniform sand.

TABLE OF CONTENTS

List of Tables	x
List of Figures	xi
CHAPTER ONE: INTRODUCTION.....	1
1.1 BACKGROUND	1
1.2 OBJECTIVES	2
1.3 ORGANIZATION	3
CHAPTER TWO: LITERATURE REVIEW.....	4
2.1 INTRODUCTION	4
2.2 STRESS WAVES IN SOILS.....	4
2.3 SMALL-STRAIN DYNAMIC PROPERTIES OF SANDY SOIL.....	7
2.3.1 Effects of Void Ratio and Mean Effective Confining Pressure on G_{max} and D_{min} of Sandy and Gravelly Soils	7
2.3.2 Effect of Grain Size Distribution on G_{max} and D_{min} of Sandy and Gravelly Soil	10
2.4 NONLINEAR DYNAMIC BEHAVIORS OF SANDY SOIL	13
2.4.1 Effects of Effective Confining Pressure and Gravel Content on G and D.....	13
2.4.2 Nonlinear Dynamic Properties of Sandy and Gravelly Soils.....	14
2.5 SUMMARY	17
CHAPTER THREE: OVERVIEW OF TESTING EQUIPMENT AND DATA ANALYSIS.....	18
3.1 INTRODUCTION	18
3.2 OVERVIEW OF RESONANT COLUMN AND TORSIONAL SHEAR EQUIPMENT	18
3.2.1 General Information.....	18
3.2.2 RCTS Confining System.....	19
3.2.3 RCTS Driving System	20
3.2.4 Specimen Height-Change Measurement.....	22
3.2.5 Motion Monitoring System.....	22

3.3	OVERVIEW OF RESONANT COLUMN AND TORSIONAL SHEAR TEST DATA ANALYSIS	24
3.3.1	Resonant Column Test Data Analysis	24
3.3.2	Torsional Shear Test Data Analysis.....	28
3.4	SUMMARY	30
CHAPTER FOUR: MATERIALS TESTED AND SAMPLE PREPARATION		31
4.1	INTRODUCTION	31
4.2	DESCRIPTION OF TEST CASES	31
4.3	DESCRIPTION OF TEST MATERIALS	35
4.4	SPECIMEN PREPARATION AND TESTING PROGRAM	43
4.4.1	Preparation of Specimens: Undercompaction Method	43
4.4.2	Test Programs	44
4.5	SUMMARY	45
CHAPTER FIVE: EFFECTS OF OVERSIZED PARTICLES ON SMALL-STRAIN DYNAMIC PROPERTIES		47
5.1	INTRODUCTION	47
5.2	UNIFORM REFERENCE SAND	47
5.2.1	Small-Strain Shear Modulus	47
5.2.2	Small-Strain Material Damping Ratio	49
5.3	EFFECTS ON SMALL-STRAIN SHEAR MODULUS OF OVERSIZED PARTICLES	55
5.3.1	Largest Oversized Particles.....	55
5.3.2	Relatively Larger and Large Oversized Particles	60
5.4	SMALL STRAIN MATERIAL DAMPING RATIO	64
5.4.1	Largest Oversized Particles.....	64
5.4.2	Relatively Larger and Large Oversized Particles	68
5.5	EFFECT OF MATERIAL TYPE	70
5.6	SUMMARY	72
CHAPTER SIX: EFFECT OF OVERSIZED PARTICLES ON NONLINEAR DYNAMIC PROPERTIES		76
6.1	INTRODUCTION	76

6.2	NONLINEAR SHEAR MODULUS	76
6.3	NONLINEAR MATERIAL DAMPING RATIO.....	79
6.4	SUMMARY	82
CHAPTER SEVEN: CONCLUSION		85
7.1	SUMMARY	85
7.2	CONCLUSION.....	86
7.2.1	Measurements in the Linear Strain Range.....	86
7.2.1.1	Shear Modulus.....	86
7.2.1.2	Material Damping Ratio.....	87
7.2.1.3	Effect of Material Type.....	88
7.2.2	Measurements in the Nonlinear Strain Range	89
7.3	RECOMMENDATION	89
REFERENCES		91
VITA.....		94

List of Tables

Table 2.1	Values of C_G and n_G of Sandy Soils (Kokusho, 1987; Ishihahra. 1996)	9
Table 4.1	Physical Properties of Washed Mortar Sand, Laird (1994)	35
Table 4.2	Physical Properties of Gravel Particles	36
Table 4.3 (a)	Specimen Properties	41
Table 4.3 (b)	Specimen Properties	41
Table 4.4	Comparison of the Weights and Volumes of Gravels for Cases C1 to C4	42
Table 4.5	Testing Schedule for RC Testing of Specimens of Sand and Sand with Gravel Particles	45

List of Figures

Figure 2.1	Propagation of Body Waves and Surface Waves in and along Surface of a Uniform, Half Space with: (a) Compression Waves, (b) Shear Waves, (c) Love Waves, and (d) Rayleigh Waves (Bolt, 1993).....	5
Figure 2.2	Comparison of Gradation Curves and the Dynamic Properties for Dense Specimens of a Poorly-Graded Sand (SP) and a Well-Graded Gravel (GW), (from Menq, 2003)	12
Figure 2.3	Comparison of Effects of Effective Isotropic Confining Pressure and Gravel Content on $G/G_{\max} - \log \gamma$ and $D - \log \gamma$ Curves of Reconstituted Gravelly Materials (Tanaka et al., 1987)	13
Figure 2.4	$G/G_{\max} - \log \gamma$ and $D - \log \gamma$ curves of Gravelly and Sandy Soils as Suggested by Seed et al. (1986).....	15
Figure 2.5	Comparison of the $G/G_{\max} - \log \gamma$ and $D - \log \gamma$ Relationships for Dense Specimens of a Poorly-Graded Sand (SP) and a Well-Graded Gravel (GW) (from Menq, 2003)	16
Figure 3.1	RCTS Testing Equipment: (a) Plan View and (b) Cross-Sectional View (from Ni, 1987)	21
Figure 3.2	Typical Dynamic Response Curve Obtained in a Small-Stain Resonant Column Test (from Stokoe et al, 1994)	24
Figure 3.3	Material Damping Ratio Measurement in RC testing using the Free Vibration Decay Curve: (a) the Free Vibrations and (b) the Log Decrement Evaluation (from Stokoe et al, 1999)	27

Figure 3.4	Calculation of shear modulus and material damping ratio using the hysteresis loop in the TS testing	29
Figure 4.1	Cross-Sectional Views of the Reference Specimens and Specimens in Cases 1 through 4 with Oversized Particles.....	33
Figure 4.2	Comparison of Actual Oversized Particle Positions (G1) in Specimen C1S (a) and in Specimen C1A (b).	34
Figure 4.3	Plan Views of Specimens in Cases C1 to C4 Showing the Positioning of the Oversized Particles at Each Level of Specimens	38
Figure 4.4	Grain Size Distribution of Specimens of Cases C1 through C8 and Uniform Reference Sand.....	39
Figure 4.5	2.8 inch Compaction Mold and Compaction Hammer	43
Figure 5.1	Comparison of the Variations of Low-amplitude Shear Modulus with Isotropic Confining Pressure from Resonant Column Tests of Uniform Sand Specimens R_1, R_2, and R_3	50
Figure 5.2	Comparison of the Variation of Low-Amplitude Shear Modulus with Isotropic Confining Pressure from Resonant Column Tests of Uniform Sand Specimens R_1, R_2, and R_3	51
Figure 5.3	Comparison of the Variations of Low-Amplitude Material Damping Ratio with Isotropic Confining Pressure from Resonant Column Tests of Uniform Sand Specimens R_1, R_2, and R_3.....	53
Figure 5.4	Comparison of the Variation of Low-Amplitude Material Damping Ratio with Isotropic Confining Pressure from Resonant Column Tests of Uniform Sand Specimens R_1, R_2, and R_3.....	54

Figure 5.5	Comparison of the Variation of Low-Amplitude Shear Modulus with Isotropic Confining Pressure from Resonant Column Tests of the Three Reference Sand Specimens, and Specimens C1S and C1A with the Largest Gravel Particle	57
Figure 5.6	Comparison of the Variations of Low-Amplitude Shear Modulus with Isotropic Confining Pressure from Resonant Column Tests of the Three Reference Sand Specimens, and Specimens C2S and C2A with the Largest Gravel Particles	59
Figure 5.7	Comparison of the Variation of Low-Amplitude Shear Modulus with Isotropic Confining Pressure from Resonant Column Tests of the Three Uniform Sand Specimens and C3S and C3A with the Relatively Larger Gravel Particles	61
Figure 5.8	Comparison of the Variation of Low-Amplitude Shear Modulus with Isotropic Confining Pressure from Resonant Column Tests of the Three Uniform Sand Specimens C4S and C4A with the Large Gravel Particle	63
Figure 5.9	Comparison of the Variation of Low-Amplitude Material Damping Ratio with Isotropic Confining Pressure from Resonant Column Tests of Specimens R_{avg} , C1S, and C1A.....	65
Figure 5.10	Comparison of the Variation of Low-Amplitude Material Damping Ratio with Isotropic Confining Pressure from Resonant Column Tests of Specimens R_{avg} , C2S, and C2A	67
Figure 5.12	Comparison of the Variations of Low-Amplitude Material Damping Ratio with Isotropic Confining Pressure from Resonant Column Tests of Specimens R_{avg} , C4S, and C4A.....	71

Figure 5.13	Comparison of the Variation of Low-Amplitude Shear Modulus with Isotropic Confining Pressure from Resonant Column Tests of Uniform Gravel Specimens (C5 through C8).....	73
Figure 5.14	Comparison of the Variation of Low-Amplitude Material Damping Ratio with Isotropic Confining Pressure from Resonant Column Tests of Uniform Gravel Specimens (C5 through C8)	74
Figure 6.1	Variation in Shear Modulus with Shear Strain at an Isotropic Confining Pressure of 18 psi from Resonant Column Tests of C1 through C4 and the Uniform Reference Sand Specimens	77
Figure 6.2	Variation in Shear Modulus with Shear Strain at an Isotropic Confining Pressure of 72 psi from Resonant Column Tests of C1 through C4 and the Uniform Reference Sand Specimens	78
Figure 6.3	Variation in Normalized Shear Modulus with Shear Strain at an Isotropic Confining Pressure of 18 psi from Resonant Column Tests of Specimens C1 through C4 and the Uniform Reference Sand Specimens	80
Figure 6.4	Variation in Normalized Shear Modulus with Shear Strain at an Isotropic Confining Pressure of 72 psi from Resonant Column Tests of Specimens C1 through C4 and the Uniform Reference Sand Specimens	81
Figure 6.5	Variation in Material Damping Ratio with Shear Strain at Isotropic Confining Pressure of 18 psi from Resonant Column Tests of Specimens C1 through C4 and the Uniform Reference Sand Specimens.....	83

Figure 6.8 Variation in Material Damping Ratio with Shear Strain at Isotropic
Confining Pressure of 72 psi from Resonant Column Tests of Specimens
C1 through C4 and the Uniform Reference Sand Specimens.....84

CHAPTER ONE

INTRODUCTION

1.1 BACKGROUND

In geotechnical earthquake engineering, the dynamic properties of soil and rock materials at shear strain below 0.5% are typically characterized by two important parameters: (1) shear modulus (G) and (2) material damping ratio (D). Understanding these two parameters is critical to the design and performance of structures and geotechnical systems that encounter dynamic loading conditions during their lifetime. The shear modulus (G) and material damping ratio (D) are determined by various types of field seismic and laboratory dynamic or cyclic measurements of the soil and rock materials.

In the past several decades, the parameters that affect the dynamic properties of sandy and gravelly soils have been researched (i.e., Hardin and Drnevich, 1972; Kokusho, 1980; Seed et al; 1986; Song, 1986; Darendeli, 2001; and Menq, 2003). They developed and strengthened empirical relationships between the dynamic properties in both the linear and nonlinear shear strain ranges and typical engineering properties such as shear strain, confining pressure, void ratio, uniformity coefficient, median grain size and so on.

The goal of this thesis research is to examine if large-sized gravel particles and their location inside specimens have a significant affect on the dynamic properties. The motivation for this study is that it is not unusual to have to perform dynamic laboratory testing of intact field samples that contain some oversized particles or test reconstituted granular samples from which a few oversized particles have been removed. To conduct this study, uniform sand was selected to form the majority of the soil specimen. Sand specimens were carefully constructed in the laboratory and a variety of rounded gravel

particles with different size were installed in the specimens during construction. In this manner, the effects of a limited number of oversized particles in specimens were studied.

1.2 OBJECTIVES

The objectives of this thesis research are follows:

1. Reconstitute uniform sand specimens with and without gravel particles and determine the dynamic properties using the combined resonant column and torsional shear (RCTS) device.
2. Investigate the effects of oversized particles on G_{\max} and D_{\min} in the linear strain range. Compare these values with those determined with uniform sand specimens to develop a general sense of potential ranges in properties a design engineer may have to consider.
3. Investigate the effects of oversized particles on G and D in the nonlinear strain range. Compare these values with those determined with uniform sand specimens to develop a general sense of potential ranges in properties a design engineer may have to consider.
4. Examine how the dynamic properties of uniform gravel specimens with different grain size characteristics compare with the sand specimens with oversized particles.
5. Offer some insight to industry on the range in values of dynamic properties that might need to be considered if the geotechnical materials contain a limited number of oversized particles.

1.3 ORGANIZATION

This thesis is organized into 7 chapters. In Chapter 2, a presentation of the basic concepts behind stress wave propagation in soils is presented. The characteristics of the various types of body waves and surface waves are described and the relationships between the stress wave properties and associated engineering properties are discussed. A brief literature review of past studies on dynamic properties of sandy and gravelly soils is given and the variety of factors that could affect the dynamic soil properties are reserved.

An explanation of the RCTS device and a brief background of the system are presented in Chapter 3. The material properties and configurations of specimens tested in this thesis research are described in Chapter 4. Results from tests performed in the RCTS device are presented in Chapters 5 and 6. In Chapter 5, the dynamic properties measured in the linear (small-strain) shear strain range are examined. The effects of the oversized particles inside the sand specimens are discussed. At the end of Chapter 5, the dynamic properties of uniform gravel specimens are discussed and compared. In Chapter 6, the dynamic properties measured within the nonlinear strain range for uniform sand specimens with and without gravel particles are presented and discussed.

This thesis is concluded in Chapter 7, in which a summary, conclusions, and recommendations are presented.

CHAPTER TWO

LITERATURE REVIEW

2.1 INTRODUCTION

Basic concepts of stress wave propagation in soil and the characteristic of dynamic soil properties are introduced in this chapter. The concepts of stress waves in soil and the principal of the wave propagation are dealt within Section 2.2. Factors that effect the small-strain dynamic soil properties are discussed in Section 2.3. The results of studies on the nonlinear dynamic behavior of soil are briefly presented in Section 2.4. A review of past studies dealing with sandy and gravelly soils that pertain to this research are also included in this chapter.

2.2 STRESS WAVES IN SOILS

The most typical way that energy generated by dynamic loading (e.g. earthquakes) is in the form of stress waves. An important characteristic of stress waves is how fast these waves propagate in soils. Because this characteristic is directly used to obtain engineering properties of soils, the stiffness and material damping ratio, it is very important to understand the characteristics of stress waves. Compression waves (P waves) and shear waves (S waves) are the two types of body waves that travel through soil. Body waves travel through the mass of soil and rock, such as the earth. For a half space, other types of stress waves also exist. Rayleigh waves and Love waves are surface waves. Surface waves travel along the soil surface due to the interaction between body waves and the surficial layers of the earth (Kramer, 1996). For example, Rayleigh waves are produced by

interaction of P or SV waves (SV waves are S waves in which the particle motion is oriented in the vertical direction). Love waves result from the interaction of SH waves (S waves in which the particles motion is horizontal and perpendicular to the direction of S wave propagation). In Figure 2.1, the direction of wave propagation (which is horizontal in this example) and the direction of particle motion are illustrated for body waves and surface waves.

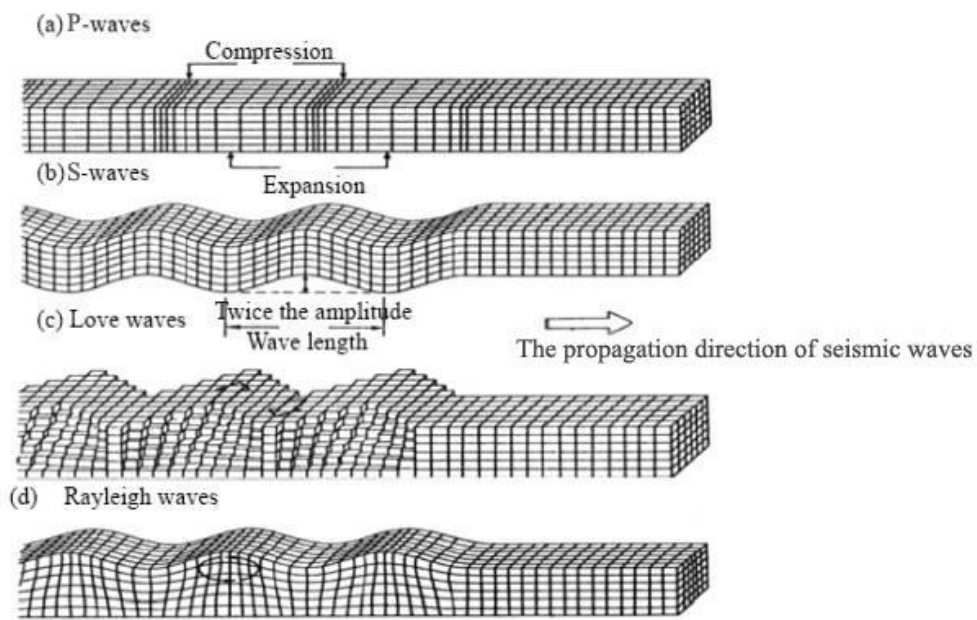


Figure 2.1 Propagation of Body Waves and Surface Waves in and along Surface of a Uniform, Half Space with: (a) Compression Waves, (b) Shear Waves, (c) Love Waves, and (d) Rayleigh Waves (Bolt, 1993)

As mentioned previously, the stiffness of a soil mass is directly related to the speed with which stress waves propagate through the soil. One classification of stiffness of soil is shear modulus, G , which can be found using a theoretical relationship between shear

wave velocity, V_s , total unit weight, γ_t , and acceleration due to gravity, g . The shear modulus, G , is given by:

$$G = \left(\frac{\gamma_t}{g}\right) V_s^2 \quad (2.1)$$

One of the primary focus of this laboratory study is on shear wave velocity measurements and shear modulus of soils. However other waveforms measured in the laboratory are of equal importance for determining dynamic properties of soils. Other stiffness classifications determined from stress wave propagation properties include Young's modulus, E , and constrained modulus, M , which are calculated by measuring unconstrained compression wave velocity, V_c , and constrained compression wave velocity, V_p , respectively as follows:

$$E = \left(\frac{\gamma_t}{g}\right) V_c^2 \quad (2.2)$$

$$M = \left(\frac{\gamma_t}{g}\right) V_p^2 \quad (2.3)$$

2.3 SMALL-STRAIN DYNAMIC PROPERTIES OF SANDY SOIL

2.3.1 Effects of Void Ratio and Mean Effective Confining Pressure on G_{\max} and D_{\min} of Sandy and Gravelly Soils

In the geotechnical engineering and earthquake engineering fields, the small-strain range (i.e. the linear range) is defined as the range of shear strain amplitudes over which the dynamic properties of soils (shear modulus, G , and material damping ratio, D) are constant. Because in that strain range the shear modulus is constant with the maximum value and the material damping ratio is constant with the minimum value. These dynamic properties are called G_{\max} and D_{\min} , respectively. In the technical literature, the small-strain range of sands is often described by strains less than 10^{-3} %. As strain increases beyond the small-strain range, the dynamic properties start to vary with the shear modulus decreasing and the material damping ratio increasing. The variation of the dynamic soil properties with strain amplitude is termed the nonlinear behavior of soils and the strain boundary between linear (i.e. small-strain range) and nonlinear strain range is referred to elastic threshold shear strain, γ_t^e . The values of elastic threshold shear strain, γ_t^e , vary depending on the dynamic and engineering characteristics of the soils and are normally determined by a dynamic testing such as resonant column (RC) and cyclic torsional shear (TS) tests.

Hardin and Richart (1963) performed dynamic tests to investigate the shear modulus of reconstituted sandy soils in the small-strain range. From their investigations, they suggested a generalized equation for G_{\max} as;

$$G_{\max} = C_G F(e) (\sigma'_o)^{n_G} \quad (2.4)$$

where C_G and n_G are constants and $F(e)$ is a function of the void ratio, e . As seen in Equation 2.4, the shear modulus is mainly a function of void ratio, $F(e)$ and isotropic effective confining pressure, σ_o' . In terms of a function of void ratio, $F(e)$, the following two forms are commonly used;

$$F(e) = \frac{(2.97 - e)^2}{1 + e} \text{ by Hardin and Black (1968)} \quad (2.5)$$

$$F(e) = 1 / (0.3 + 0.7e^2) \text{ by Hardin (1978)} \quad (2.6)$$

Hardin and Black (1968) also found that the small-strain shear modulus is proportional to the half power of isotropic effective confining pressure for most clean sand; hence $n_G = 0.50$ in Equation 2.4. With regards to the constant values of C_G and n_G , several values have been suggested by researchers and these values are presented in Table 2.1. As shown in the table, the values of C_G ranges from 3300 kPa to 9000 kPa and the n_G , the exponent of σ_o' is generally close to 0.5.

The small-strain material damping ratio in shear, $D_{s,min}$, has been difficult to measure accurately due to background noise and equipment-generated damping which has often not be taken into account. In spite of those difficulties, Laird (1994) suggested that the value of $D_{s,min}$ could be determined by;

Table 2.1 Values of C_G and n_G of Sandy Soils (Kokusho, 1987; Ishihahra, 1996)

Referebce	F (e)	C_G (kPa)	n_G	Soil description
Hardin and Richart (1963)	$\frac{(2.17-e)^2}{1+e}$	7000	0.5	Round grain Ottawa sand
	$\frac{(2.97-e)^2}{1+e}$	3300	0.5	Angular grained crushed quartz
Iwasaki et al. (1978)	$\frac{(2.17-e)^2}{1+e}$	9000	0.38	Eleven kinds of clean sand
Kokusho (1980)	$\frac{(2.17-e)^2}{1+e}$	8400	0.5	Toyoura sand
Yu and Richart (1984)	$\frac{(2.17-e)^2}{1+e}$	7000	0.5	Three kinds of clean sand

$$D_{s,\min} = C_D F(e) (\sigma'_o)^{n_D} \quad (2.7)$$

where: $D_{s,\min}$ = small-strain material damping ratio,

C_D = dimensionless material damping ratio coefficient,

n_D = effective isotropic stress exponent, and

$$F(e) = 1/(0.3 + 0.7e^2).$$

This equation indicates that the factors of void ratio and isotropic effective confining pressure play important roles in the determination of material damping ratio as well as shear modulus in the small-strain range.

2.3.2 Effect of Grain Size Distribution on G_{\max} and D_{\min} of Sandy and Gravelly Soil

Even though Hardin and Richart concluded that the effects of grain size distribution characteristics, including median grain size, D_{50} , and uniformity coefficient, C_u , were included in the effect of void ratio on the dynamic properties, they did not show any relationships of those characteristics with dynamic properties. However, Menq (2003) tested 59 reconstituted gravelly and sandy soils using equipment he developed at the University of Texas at Austin. This equipment is a large scale, multi-mode, resonant column device (MMD). In addition he used the combined resonant column and torsional shear test device (RCTS) in the Soil and Rock Dynamics Laboratory. In his study, Dr. Menq investigated the effects of grain size distribution characteristics on the small-strain shear modulus of gravelly and sandy soils. He related the effect of median grain size, D_{50} and uniformity coefficient, C_u among the grain size distribution characteristics. He modified the equation of Hardin and Richart (1963) and suggested this modified equation can be expressed as:

$$G_{\max} = C_{G3} \times C_u^{b1} \times e^x \times \left(\frac{\sigma'_o}{P_a}\right)^{n_G} \quad (2.8)$$

where: $C_{G3} = 67.1$ MPa (1400 ksf), which is G_{\max} at 1 atm for a material with e and C_u

both equal to 1,

$b1 = -0.2$,

$e =$ void ratio,

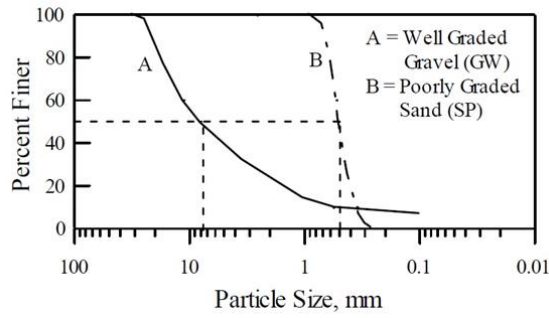
$x = -1 - (D_{50}/20)^{0.75}$, and

$$n_G = 0.48 \times C_u^{0.09}$$

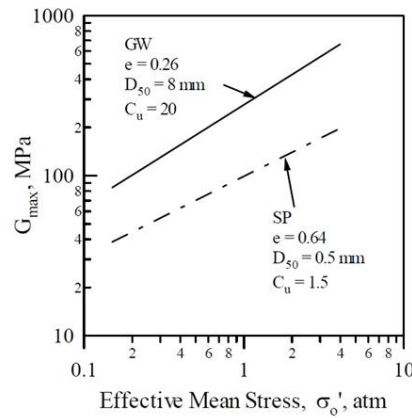
Indicating that D_{50} affects void ratio function and uniformity coefficient, C_u affects both the sensitivity of the soil to the effective isotropic confining pressure, n_G , and small-strain shear modulus at one atmosphere, A_G .

On the other hand, he did not find any strong correlation between grain size distribution characteristics and small-strain material damping ratio, $D_{s, \min}$. Dr. Menq did show that there was more variability in the general trends of $D_{s, \min}$ which he associated with the more complexities that arise in measuring the material damping ratio, D .

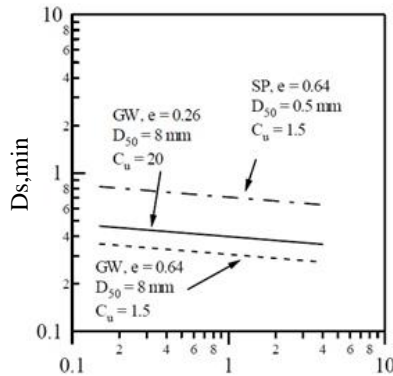
As a result of his testing, Dr. Menq found that the small-strain shear modulus, G_{\max} , of the very dense, well-graded gravel is about 1.5 times higher than that of the poorly-graded sand. This finding indicates that the decrease in uniformity and increase in the median grain size could mainly cause the increase in G_{\max} . Moreover, he noted that the G_{\max} of the well-graded gravel increases more rapidly than that of the poorly graded sand as effective confining pressure increases. For material damping ratio in his model, the $D_{s, \min}$ of well-graded gravel is lower than that of the poorly-graded fine sand due to the effect of particle size. Comparisons of these relationship of dynamic properties and affecting factor such as D_{50} , C_u and e of poorly graded fine sand (SP) and the well graded gravel (GW) as well as gradation curves of both soils are presented in Figure 2.2.



(a) Gradation Curves of GW and SP Soil



(b) Log G_{max} – log σ'_o Relationships of GW and SP Soils



(c) Log $D_{s,min}$ – log σ'_o Relationships of GW and SP Soils

Figure 2.2 Comparison of Gradation Curves and the Dynamic Properties for Dense Specimens of a Poorly-Graded Sand (SP) and a Well-Graded Gravel (GW), (from Menq, 2003)

2.4 NONLINEAR DYNAMIC BEHAVIORS OF SANDY SOIL

2.4.1 Effects of Effective Confining Pressure and Gravel Content on G and D

Tanaka et al. (1978) tested a gravelly soil reconstituted to investigate the nonlinear behavior. They found that the isotropic effective confining pressure and gravel content mainly affected the shear modulus and material damping ratio as strain increases. Especially as the confining pressure increases, the gravelly soil behave more linearly for both shear modulus and material damping ratio, and the linearity are more apparent in the reconstituted soil with less gravel content (Figure 2.3).

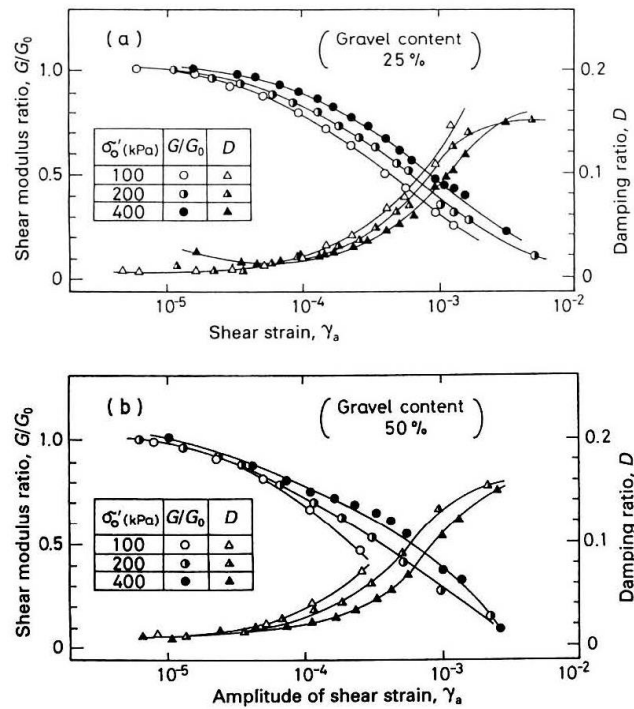
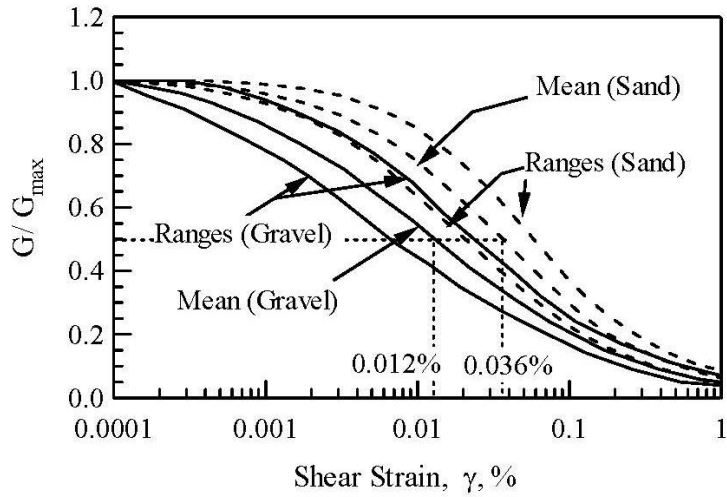


Figure 2.3 Comparison of Effects of Effective Isotropic Confining Pressure and Gravel Content on $G/G_{\max} - \log \gamma$ and $D - \log \gamma$ Curves of Reconstituted Gravelly Materials (Tanaka et al., 1987)

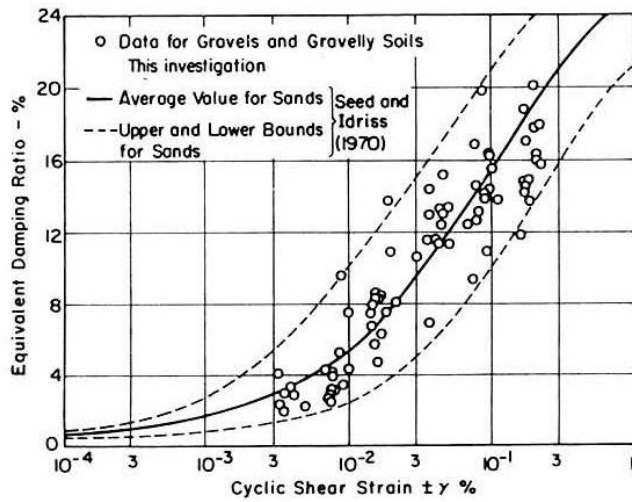
When it comes to comparisons of nonlinearity, the concept of reference strain, γ_r , is very useful. Reference strain is the strain at which the G/G_{\max} is 0.5. Seed et al. (1986) suggested that the nonlinear dynamic behavior of sandy soils is less than that of gravelly soils as seen in Figure 2.4. In the figure, the reference strain of the mean $G/G_{\max} - \log \gamma$ curves for sandy and gravelly soils are 0.036 % and 0.012 %, respectively. This trend agrees well with the overall trend by Tanaka et al. (1987); that is, the soils with less gravel content behave more linearly and this trend is more easily shown by the reference strain. The reference strain of sandy soil is higher than that of gravelly soils. On the other hand, Seed et al. (1986) determined a wide range of material damping ratios of sandy soil in terms of nonlinear behavior and showed that the material damping ratio of most gravelly soils are included in the range.

2.4.2 Nonlinear Dynamic Properties of Sandy and Gravelly Soils

Menq (2003) summarized test results of comparisons between well-graded gravel and poorly-graded fine sand as shown in Figure 2.5. He used the modified hyperbolic model (Darendeli, 2001) to study values of reference strain, γ_r , curvature coefficient, a , and their relationships with grain size distribution characteristics. Dr. Menq found that the shear modulus, G , of well-graded gravel in the nonlinear range is larger than that of poorly graded fine sand due to the effect of higher C_u and D_{50} values indicating that the grain distribution characteristic have influences on the nonlinear soil behaviors of sandy and gravelly soils. Additionally the reference strain of GW is smaller than that of SP due to the increase of C_u (Figure 2.5) indicating that the grain distribution characteristics have an effect on the nonlinear behavior of sandy and gravelly soils and are necessary in modeling the dynamic properties. With respect to material damping ratio, the values of



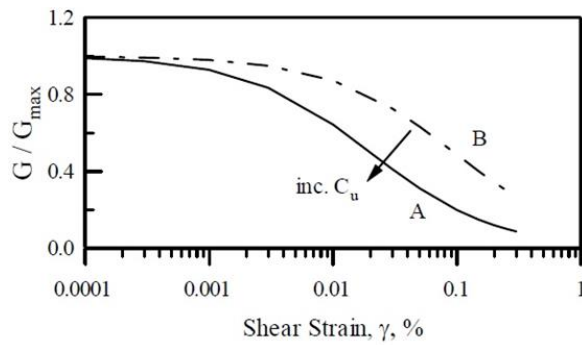
(a) Normalized Shear Modulus in Nonlinear Range



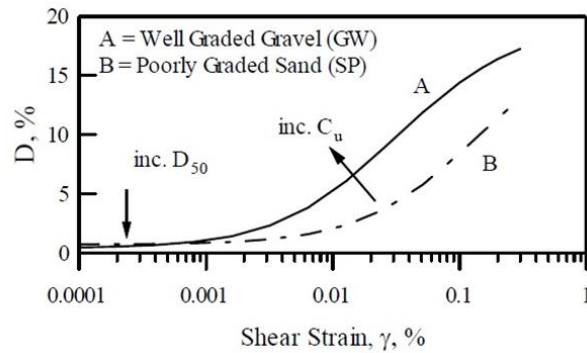
(b) Material Damping Ratio in Nonlinear Range

Figure 2.4 $G/G_{max} - \log \gamma$ and $D - \log \gamma$ curves of Gravelly and Sandy Soils as Suggested by Seed et al. (1986)

material damping ratio of SP in the small strain range are larger than those of GW over the elastic threshold shear strain, γ_t^e . However, in the nonlinear range (Figure 2.5(b)), the nonlinear D values of gravels are much larger than sand.



(a) $G/G_{max} - \log \gamma$ Relationship



(b) $D - \log \gamma$ Relationship

(c)

Figure 2.5 Comparison of the $G/G_{max} - \log \gamma$ and $D - \log \gamma$ Relationships for Dense Specimens of a Poorly-Graded Sand (SP) and a Well-Graded Gravel (GW) (from Menq, 2003)

2.5 SUMMARY

The relationship between dynamic material properties and the characteristics of stress wave propagation through the earth have researched. The small-strain stiffness in shear, G_{\max} , is best estimated by measuring the shear wave velocity (V_s). The level of shearing strain is one of key factors that affect the nonlinear dynamic properties of sandy and gravelly soil materials. Menq (2003) developed empirical relationships between the grain size characteristics and dynamic soil properties in shear (G and D) both in the linear and nonlinear ranges. The less uniform (expressed by higher values of C_u) a sandy or gravelly soil is, the more sensitive the material is to confining pressure changes in the small-strain range and the more nonlinear the material behave in the larger-strain range. The median grain size has been forward to also be important to the small-strain shear modulus at one atmosphere.

CHAPTER THREE

OVERVIEW OF TESTING EQUIPMENT AND DATA ANALYSIS

3.1 INTRODUCTION

In this chapter, an overview of the combined resonant column and torsional shear test (RCTS) device. The analysis method used to determine the dynamic soil properties of from RCTS testing is discussed. The combined RCTS test is a robust way of determining dynamic properties such as shear modulus, G and material damping ratio, D of sandy and gravelly soils. The purpose of the RCTS testing in this thesis research is to evaluate and advise effects of oversized particles on the dynamic measurements. In Section 3.2, the general information about the RCTS equipment is presented. The methodology of analyzing the results from the RCTS test is outlined in Section 3.3.

3.2 OVERVIEW OF RESONANT COLUMN AND TORSIONAL SHEAR EQUIPMENT

3.2.1 General Information

The combined resonant column and torsional shear (RCTS) equipment was developed over several decades by Prof. Stokoe and his students (Isenhower, 1979; Lodde, 1982; Ni, 1987; and Kim, 1991) in the Soil and Rock Dynamics Laboratory at the University of Texas at Austin. The RCTS approach is a very useful means of evaluating the dynamic material properties in terms of shear modulus and material damping ratio, G and D , respectively. The RCTS equipment is annually checked for calibration compliance due to the NQA-1 studies upon which it is used. As a result, the equipment and

accompanying experience make these measurements well suited for this study. The combined RCTS is made up of four systems which are: (1) a confining system allowing for modeling a variety of confinement conditions, (2) a driving system capable of loading torsional excitation, (3) a specimen height-change monitoring system used during confinement, and (4) a slow-cyclic and dynamic motion-monitoring system. The overall device is controlled by a microcomputer system (Ni, 1987) with automated data acquisition and processing.

3.2.2 RCTS Confining System

The confining system chamber consists of one hollow cylinder, two end plates and four or six rods that are used to connect the top and bottom end plates. This system is made of stainless steel. One reason for using stainless steel is to eliminate the possibility of magnetic reactions between the confining system and the magnets attached to the drive plate used in the driving system. The confining system is capable of handling pressure up to 450 psi. The pressure inside of the cell is regulated for isotropic confining by either using a Fairchild model 44-2200 regulator from 2 to 90 psi or a Tescom 44-2200 model regulator from 80 to 500 psi. The source of air (or other gas) pressure is the building supply pressure up to about 75 psi or nitrogen gas from a high-pressure “bottle” up to 450 psi. On the bottom plate, a metal base pedestal is fixed with 4 to 6 screws. The soil and rock specimen is placed on the base pedestal. A top cap is placed on the specimen and a membrane is placed around the specimen. The surface of both top cap and base pedestal are rough so that slippage does not occur. The pore water or pore air pressure inside the specimen is vented to room pressure through a drainage line that is open during testing so that the generation of pore water during testing can be release.

In this research, the sandy and gravelly specimens were built by compacting them on the base pedestal. The sandy and gravelly specimens had a nominal diameter of 2.8-inches and a nominal height about twice the diameter. A proper-sized membrane was placed around specimen. On the membrane that was rolled on to the top cap and base pedestal, vacuum grease and O-rings were used to seal the specimen from the confining air pressure.

3.2.3 RCTS Driving System

The driving system is composed of a four armed aluminum drive plate, four permanent rectangular magnets, and four sets of drive coils in which each set of drive coils consists of two drive coils shaped in the form of an ellipse to surround each end of the permanent magnet (Figure 3.1). The four permanent magnets are attached to four different arms on the drive plate. A voltage signal from a power source that includes a function generator and a power amplifier passes through the drive coils. Torsional motion is generated and the level of torque depends on; the strength of magnets, dimensions of drive coils, electro-magnetic characteristic of drive coils, width of gap between magnet and drive coil, and finally characteristics of powering equipment. The operator manually assigns the powering equipment a certain value and range of input voltage and frequency sweeping range using the microcomputer. In this study, the resonant column portion of the combined RCTS system was operated using a logarithmic-linear frequency sweep of sinusoidal voltage. Once the target input voltage and sweeping level were determined, RC testing was conducted: (1) using a rough sweep to roughly find the resonant frequency, (2) then using a fine sweep to precisely determine the resonant frequency, and finally (3) free vibration decay testing.

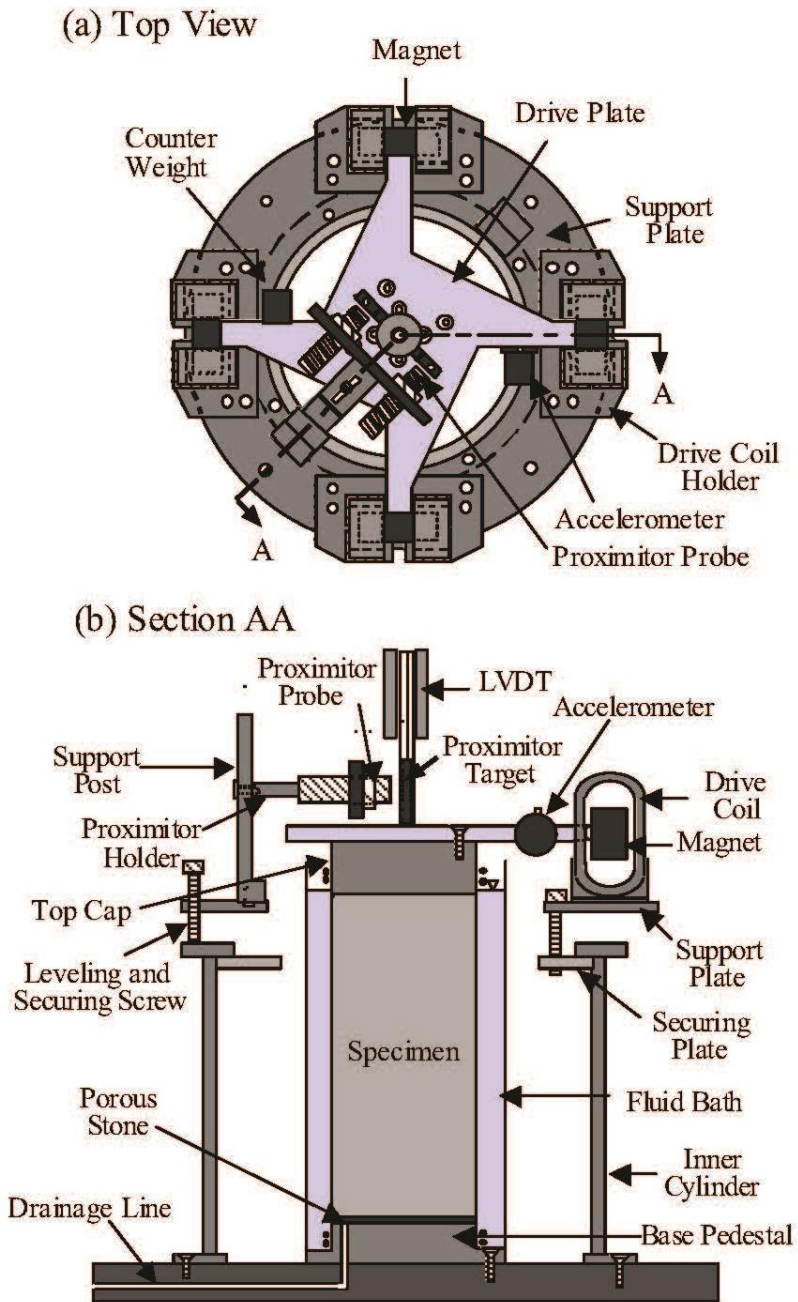


Figure 3.1 RCTS Testing Equipment: (a) Plan View and (b) Cross-Sectional View (from Ni, 1987)

3.2.4 Specimen Height-Change Measurement

To monitor the height change of the specimen due to consolidation or compaction during confinement, a linear variable differential transducer (LVDT) is used. The change in height of the specimen during testing is important because it allows estimates to be made of the change in void ratio, total unit weight, and height of the specimen which are needed in the data reduction.

As seen at Figure 3.1 (b), the LVDT core is attached to the center of the drive plate so that the LVDT coil housing which surround the core does not physically touch the LVDT core. The change in output voltage of LVDT is automatically recorded by the microcomputer system and the initial specimen height is corrected using a pre-determined calibration factor.

3.2.5 Motion Monitoring System

As mentioned earlier, the combined RCTS system can operate as two independent types of tests: (1) a torsional resonant column test (RC), and (2) a slow-cyclic torsional shear test (TS). Both types of test are performed on the same specimen at any desired time. However, these tests have an important difference in that each test measures the values of G and D in a different frequency range. For instance, in the RC test, measurements are performed in the relatively high frequency range (20 ~ 200 Hz). On the other hand, the TS test involves cycling in the low frequency (0.1 ~ 10 Hz). As a result, the motion monitoring systems are different for each type of test (Ni, 1987).

First of all, because the RC testing involves relatively high frequency motions, accelerometer is used as the motion monitoring sensor. The motion signals in torsional loading of specimen are monitored by an accelerometer attached to the drive plate (see

Figure 3.1). The accelerometer signal is conditioned with an associated charge amplifier. The conditioned signal is monitored with a voltmeter and oscilloscope and finally the microcomputer generates a dynamic response of motion vs. frequency and the strain amplitude is calculated. Based on the dynamic response curve, the resonant frequency and peak shear strain amplitude are determined as shown in Figure 3.2. Additionally the half power band width method is used to calculate material damping ratio at small-strain which the free-vibration decay method is used at larger strains. More details about the data analysis are presented in the next section.

In the TS test which involves low-frequency excitation, a proximator displacement sensor is used as the motion sensor. A proximator is a distance measuring sensor that is used to determine the change in width of the air gap between the probe and the associated target due to a torque-twist motion at the top of the specimen. This monitoring system is composed of two proximator probes, a U-shaped target, a regulated DC power supply, and so on. The output signals of the probes through the regulated DC power supply, DC shifter, and OP amplifier are captured by the microcomputer system and are used to create a shear strain-shear stress hysteresis loop. Based on that hysteresis loop, the shear modulus and damping ratio are determined by the slope and the area of the hysteresis loop, respectively. More details about the TS data analysis procedures are discussed in the next section.

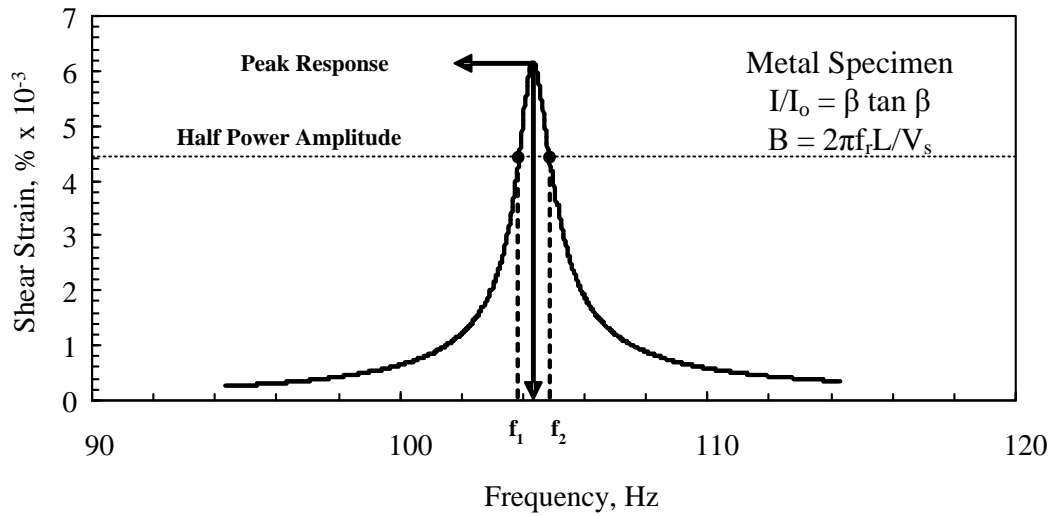


Figure 3.2 Typical Dynamic Response Curve Obtained in a Small-Strain Resonant Column Test (from Stokoe et al, 1994)

3.3 OVERVIEW OF RESONANT COLUMN AND TORSIONAL SHEAR TEST DATA ANALYSIS

3.3.1 Resonant Column Test Data Analysis

As mentioned previously, the output signal from the soil specimen due to the drive plate excitation is recorded by the monitoring system (Section 3.2.2). The result is that a dynamic response curve in the frequency domain is obtained as shown in Figure 3.2. This response curve is critical in determining the resonant frequency of the specimen and the peak shear-strain amplitude. Normally, the shape of the dynamic response curve under the small-strain loading is bell-shaped as on the Figure 3.2. The determined resonant frequency (transformed from a circular resonant frequency as multiplied by 2π) is used to calculate a shear wave velocity by following equation:

$$\frac{I}{I_0} = \frac{\omega_r \times \ell}{V_s} \tan \frac{\omega_r \times \ell}{V_s} \quad (3.1)$$

where: I = mass polar moment of inertia of the soil specimen,

I_0 = mass polar moment of inertia of the top cap and drive system,

ω_r = circular resonant frequency ($\omega_r = 2\pi f_r$),

ℓ = length of the soil specimen, and

V_s = shear wave velocity of the soil specimen.

Because wave properties are easily transformed to stiffness properties with material total unit weight and gravitational acceleration (see Chapter 2), the shear modulus is easily calculated from the response curve once V_s is determined. The material damping ratio of the specimen can also be determined from the response curve using the half-power band width method if testing is conducted in the linear range. The theoretical relationship is (Van Hoff, 1993):

$$D = \frac{f_1 - f_2}{2f_r} \quad (3.2)$$

where: $f_{1,2}$ = the lower and upper frequencies at which the shear strain amplitude is equal to the half power peak amplitude ($0.707A_{\max}$),

f_r = the resonant frequency of the specimen, and

A_{\max} = the amplitude at f_r .

Furthermore, the material damping ratio is also obtained from free-vibration-decay curve as illustrated in Figure 3.3. The measurement is performed separately from the frequency sweeping tests. After finishing the fine-sweep test for determination of the dynamic response curve, the drive plate is excited at the resonant frequency with the same voltage at which the peak shear strain was measured. The excitation level is continued until steady-state motion is achieved after which the system power is suddenly shut off. The specimen then vibrates freely and the free-vibration decay is recorded by the microcomputer system. The decay of shearing strain amplitude during this free vibration occurs naturally. The decay from two (or more) successive strain amplitudes of motion (Z_1 and Z_2) is used to calculate the logarithmic decrement (δ):

$$\delta = \ln\left(\frac{Z_1}{Z_2}\right) \quad (3.3)$$

The curve of the log strain amplitude vs. number of cycles of motion is shown in Figure 3.3 (b) for small-strain measurements in the linear range. From the log decrement, the material damping ratio (D) is calculated as:

$$D = \frac{\delta}{\sqrt{4\pi^2 + \delta^2}} \quad (3.4)$$

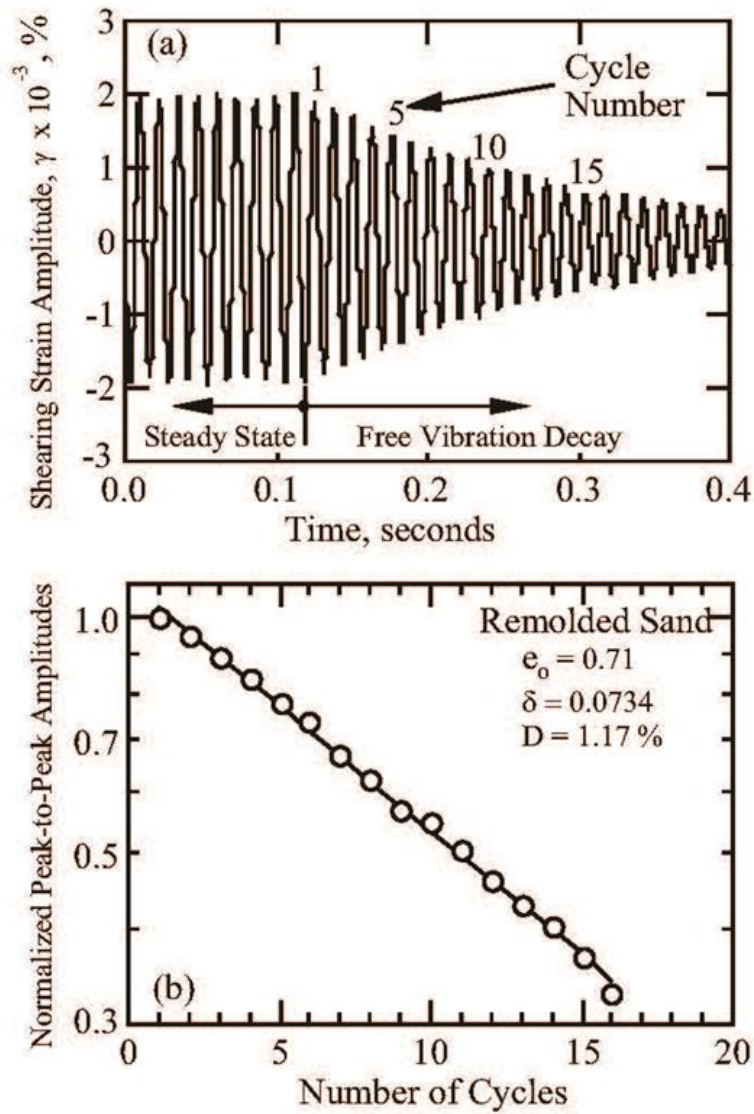


Figure 3.3 Material Damping Ratio Measurement in RC testing using the Free Vibration Decay Curve: (a) the Free Vibrations and (b) the Log Decrement Evaluation (from Stokoe et al, 1999)

3.3.2 Torsional Shear Test Data Analysis

One of the advantages of the combined RCTS is that it is possible to run a slow-cyclic torsional shear tests separately with the torsional resonant column test. The main purpose of cyclic torsional shear tests is to obtain a stress-strain relationship referred to as a torque-twist hysteresis loop. The shear stress in the TS testing is calculated by:

$$\tau_{\text{avg}} = r_{\text{eq}} \times \frac{T}{J_p} \quad (3.5)$$

where: τ_{avg} = the average value of shearing stress,

r_{eq} = equivalent radius of the specimen,

T = the value of torque applied to the specimen, and

J_p = area polar moment inertia of the specimen.

The excitation frequency in the TS test is in the range of 0.1 Hz ~ 10 Hz so it is relatively slow compared to the RC test. Therefore, by comparing both tests, it is possible to evaluate the effect of excitation frequency on the dynamic properties of the material being tested. Basically the shearing strain, γ , from the TS test is calculated using the calibration factor so that the hysteresis loop is drawn with shear stress, τ , versus shear strain, γ (Figure 3.4). For hysteresis loop in the figure, the slope of the loop represents the secant shear modulus and the ratio of area of triangle, A_T to the area of the hysteresis loop allows determination of the material damping ratio as:

$$D = \frac{1}{4\pi} \times \frac{A_L}{A_T} \tag{3.6}$$

where: D = material damping ratio of the specimen,

A_L = area within the hysteresis loop, and,

A_T = area of the triangle formed by the secant modulus line and the γ -axis

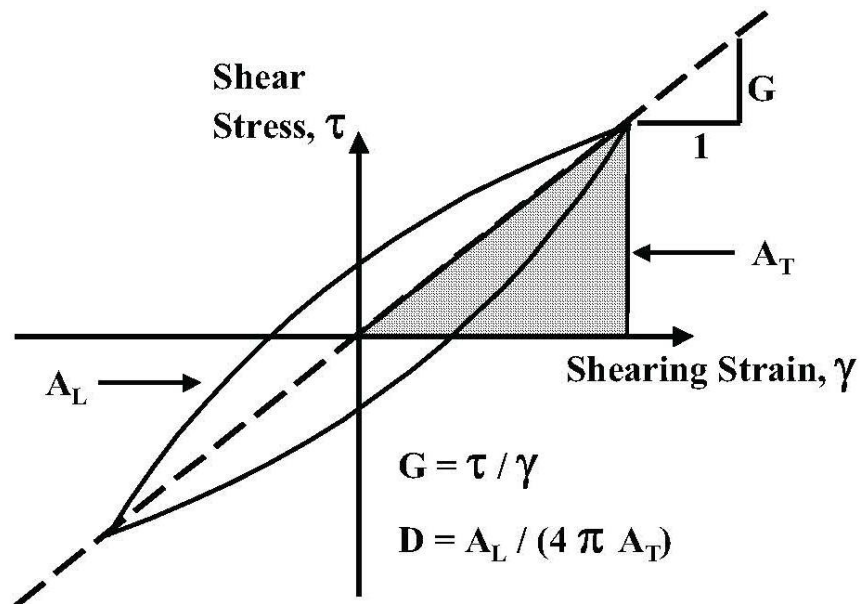


Figure 3.4 Calculation of shear modulus and material damping ratio using the hysteresis loop in the TS testing

It is important to note that the process of obtaining the material damping ratio from both the half-power bandwidth method and the free vibration decay curve in the RC test as well as obtaining the material damping ratio in the TS test from the hysteresis loop include equipment-generated damping (Hwang, 1997, Menq, 2003). Therefore, it is critical that determination of equipment-generated damping associated with each system and test method be evaluated before proceeding with each testing.

3.4 SUMMARY

The combined RCTS device was used to measure both shear modulus and material damping ratio in the linear and nonlinear ranges in this thesis research. Measurements were performed on sandy soil specimens with and without gavel particles. An overview of the equipment and data analyses procedures is presented in this chapter before discussing the material tested and test results.

CHAPTER FOUR

MATERIALS TESTED AND SAMPLE PREPARATION

4.1 INTRODUCTION

The goal of this study is to determine how oversized particles inside a uniform sand specimen affect the cyclic and dynamic properties; that is, the shear modulus (G) and material damping ratio (D). Several sizes of gravel were used as oversized particles in a uniform sand. The gravel particles were arranged in several special arrangements as described in Section 4.2. Details about physical and engineering properties of the uniform sand and the gravel particles are presented in Section 4.3. Finally, a methodology of preparing the specimens and a testing program with the RCTS device are explained in Section 4.4.

4.2 DESCRIPTION OF TEST CASES

Before describing specimens containing oversized particles, measurements of the dynamic properties of the uniform sand were first performed. To examine possible variability in G and D due to construction on uniform sand specimens, three “identical” washed mortar sand specimens (R_1 , R_2 , and R_3 , respectively) were compacted and tested in the RCTS device. The identifier of the specimens, R , stand for “Reference”, meaning these specimens play the important role of representing the control case. The

number following the letter R simply represents the specimen number with these control specimens built.

Besides the three uniform sand specimens (R_1, R_2, and R_3), eight specimens cases (C1 through C8) were considered with oversized particles in this study. These eight cases are: (1) C1 to C4 in which the effects of sizes, numbers, and locations of the oversized particles were examined, (2) C5 to C7 in which three uniform gravel specimens with different median grain sizes were evaluated, and (3) C8 which had a unique mixture specimen of the uniform sand and one of the uniform gravels. Cases C1 through C4 are each composed of two sub-cases, depending on the symmetrical or asymmetrical location of the oversized particles.

Figure 4.1 summarized identifications (ID.) and configurations of all specimens for C1 to C4 as well as the three uniform sand specimens of R_1, R_2, and R_3. A cross-section view of each specimen is shown. For example, C1 (CASE 1) which consisted of Specimen C1S (symmetrical specimen of C1) and Specimen C1A (asymmetrical specimen of C1) indicating that these two specimens have same kind of oversized particle (G1, meaning gravel particle No.1), but the locations of the particle are different. In Case C1, Specimen C1S has an oversized particle of G1 at the axis of rotation, inducing a symmetrical situation. On the other hand, Specimen C1A has the same particle (G1) offset laterally from the vertical, longitudinal axis of the specimen which leads to specimen asymmetry. A discussion of the engineering characteristics of the oversized particles is presented in the next section.

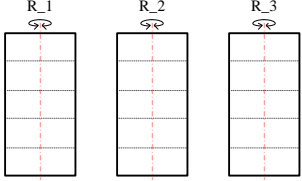
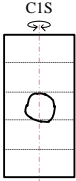

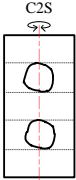

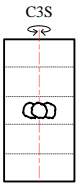

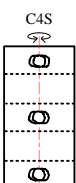

Case ID.	Symmetrical Soil Matrix, SSM	Asymmetrical Soil Matrix, ASM
Reference (R)		
CASE 1 (C1S and C1A)		
CASE 2 (C2S and C2A)		
CASE 3 (C3S and C3A)		
CASE 4 (C4S and C4A)		

Figure 4.1 Cross-Sectional Views of the Reference Specimens and Specimens in Cases 1 through 4 with Oversized Particles

All specimens in this study were reconstituted a diameter of 2.8 inches (71 mm) and a height of 5.6 inches (142 mm). Photographs of the installation of the oversized particle (G1) in Specimen C1S (left hand side) and in Specimen C1A (right hand side) are presented in Figure 4.2 (a) and 4.2 (b), respectively. As seen, the oversized particle (G1) occupies about 20% of the cross-sectional area of each specimen. However, the location of particle G1 is difference between the specimens. This difference in the location inside of specimens would not change the values of parameters such as median grain size (D_{50}), initial void ratio (e_0), and uniformity coefficient (C_u), which play critical roles in predicting the dynamic properties of stiffness and material damping ratio. However, this variation in the size and location of a few large particles is unknown even though intact soil specimens are often tested with this condition; hence it is worthwhile examining this condition under controlled laboratory situations.

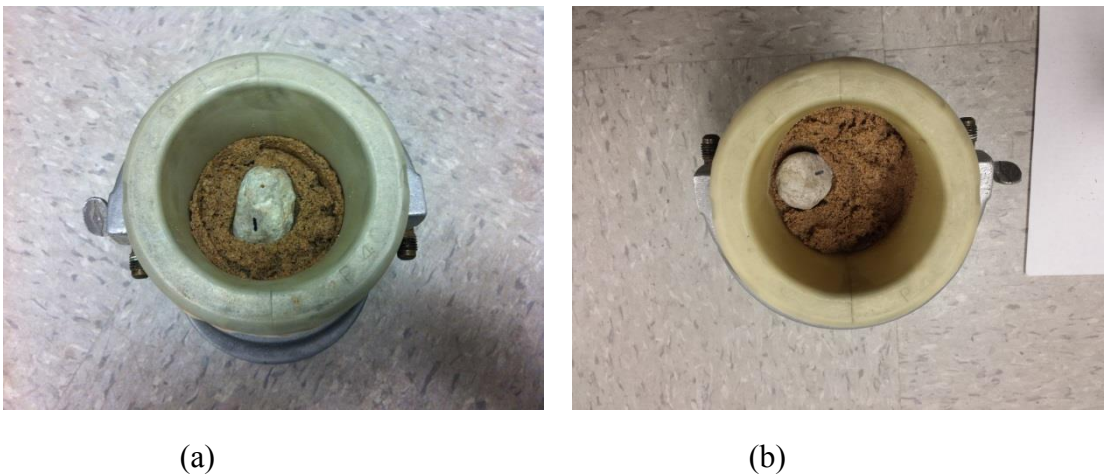


Figure 4.2 Comparison of Actual Oversized Particle Positions (G1) in Specimen C1S (a) and in Specimen C1A (b).

4.3 DESCRIPTION OF TEST MATERIALS

Washed mortar sands have been investigated in the Soil and Rock Dynamics Laboratory at the University of Texas at Austin for decades (Ni 1987, Kim 1991, and Laird 1994). The sand is easily obtained from the flood plain of the Colorado River in Austin, Texas. General physical properties of washed mortar sand are provided in the Table 4.1. As shown in the table, basically this sand is classified as poorly-graded fine sand (SP) by the Unified Soil Classification System, USCS (ASTM D-2487). The approximate minimum void ratio is about 0.56. The approximate maximum void ratio is about 0.84. The sand used in this study has D_{50} of about 0.01 inches, and C_u of about 1.7 and less than about 1 % fines.

Table 4.1 Physical Properties of Washed Mortar Sand, Laird (1994)

Unified Soil Classification	SP
Grain Character	Sub-angular to sub-rounded
Soil Composition	40% Quartz 30% Feldspar 20% Other Minerals 10% Shell Fragments
Specific Gravity	2.67
Maximum Dry Density	106.6 pcf (16.7 kN/m ³)
Minimum Dry Density	90.6 pcf (14.2 kN/m ³)
Maximum Void Ratio	0.839
Minimum Void Ratio	0.563
<i>Particle Size Distribution:</i>	
Median Grain Size, D_{50}	0.35 mm
Effective Grain Size, D_{10}	0.25 mm
$C_u, (D_{60}/D_{10})$	1.71
$C_z, (D_{30})^2 / (D_{60} * D_{10})$	1.19
% Passing #200 Sieve	< 1%

In addition to the characteristics of the washed mortar sand, the physical properties of the oversized particles used in this study were investigated (see Table 4.2). As seen in the table, all 14 oversized particles (G1 through G14) can be grouped into three categories; (I) “largest” oversized particles (G1 and G2), (II) “relatively larger” oversized particles (G3 through G5), and (III) “large” oversized particles (G6 through G14). Recommendations of the maximum particle size that can be tested in reconstituted sand specimens is a particle diameter of about one sixth of the specimen diameter (ASTM D 4105). For the specimen diameter of 2.8 inches, the one-sixth size is about 0.47 inches, which is about a half inches. The estimated average diameter in each category of oversized particles exceeded the recommended maximum particle size of 0.47 inches. In other words, all oversized particles were selected for the purpose of this study. (The effect of oversized particles on the dynamic properties.) The unit weights of the particles were estimated by measuring directly the weights of particles and the volume of the particles by the volume of water they displaced in a graduated beaker.

Table 4.2 Physical Properties of Gravel Particles

Group ID.	Largest Oversized Particles (I)		Relatively Larger Oversized Particles (II)			Large Oversized Particles (III)								
Gravel ID.	G1	G2	G3	G4	G5	G6	G7	G8	G9	G10	G11	G12	G13	G14
Average Estimated Diameter (in.)	1.3	1.3	0.9	0.8	0.8	0.7	0.7	0.6	0.6	0.7	0.6	0.7	0.6	0.6
Volume (in ³)	0.85	0.92	0.10	0.17	0.10	0.12	0.13	0.13	0.12	0.10	0.09	0.24	0.23	0.20
Unit Weight (g/cm ³)	2.60	2.63	2.68	2.56	2.62	2.46	2.58	2.54	2.68	2.57	2.62	2.49	2.56	2.56
Unit Weight (pcf)	162.4	164.2	167.5	159.5	163.4	153.5	161.2	158.6	167.0	160.6	163.8	155.1	160.0	160.1

In Figure 4.3, plain views of the general locations of the oversized particle for Cases C1 to C4 are presented. All particles in this figure were scaled proportionally to the diameter of specimen (2.8 inches), so that the size and relative locations can be more effectively and visually compared. The axis of rotation is also marked on each specimen with a small “+” (Center Point). As seen in the figure, Cases C1 and C2 involved the “largest” particles (G1 and G2), Cases C3 and C4 had the “larger” (G3 to G5) and “large” (G6 to G14) particles, respectively. The symmetrical specimens were shown in the left column and the asymmetric specimens are shown in the right column. Even though G1 and G2 are the largest individual particles, Specimen C3S has the largest concentrated area of an equivalent oversized particle and Specimen C4S has the second largest concentrated area of an equivalent oversized particle.

Grain size distribution tests were performed in accordance with ASTM D422-63 for all specimens. The grain size distribution curves for each specimen are shown in Figure 4.4. As seen, the curves for the specimens in Cases C1 through C4 are reasonably similar, with the difference in the large particle sizes. The uniform sand specimen (R) and the specimens in Cases C1, C2 and C3 are quite similar. The similarity of the grain size distribution curves implies that the effect of the oversized particles characterized by the sieve analyses and accompanying parameters (i.e., D_{50} , C_u and so on) may not be strong indicators of potential effects on the measured dynamic properties. Uniform gravel specimens C5 to C7 that were tested and also shown in Figure 4.4. These specimens represent large-grained uniform material as shown by the steep slope of each curve. Specimen C8 has a gap-graded distribution and includes about 50% gravel and 50% sand.

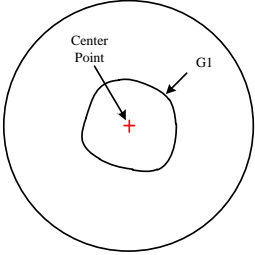
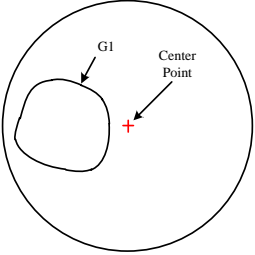
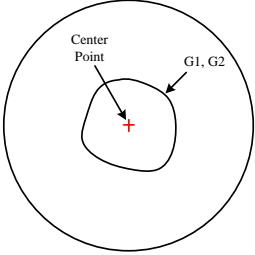
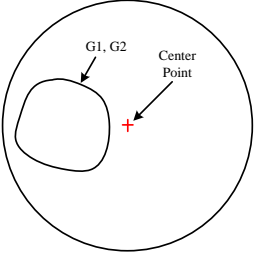
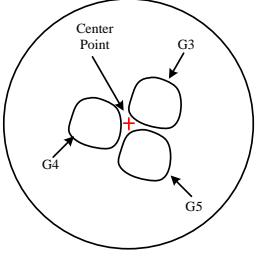
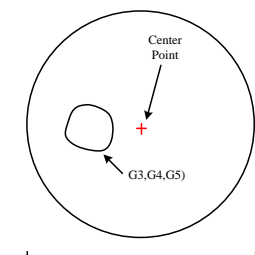
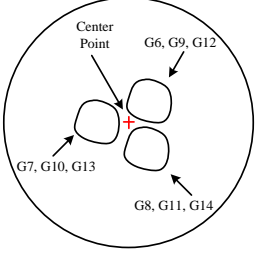
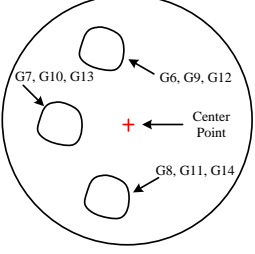
Case ID.	Symmetrical Soil Matrix, SSM	Asymmetrical Soil Matrix, ASM
<p>CASE 1 (C1S and C1A)</p>	 <p>2.8-in.(71.12 mm) Diameter</p>	 <p>2.8-in.(71.12 mm) Diameter</p>
<p>CASE 2 (C2S and C2A)</p>	 <p>2.8-in.(71.12 mm) Diameter</p>	 <p>2.8-in.(71.12 mm) Diameter</p>
<p>CASE 3 (C3S and C3A)</p>	 <p>2.8-in.(71.12 mm) Diameter</p>	 <p>2.8-in.(71.12 mm) Diameter</p>
<p>CASE 4 (C4S and C4A)</p>	 <p>2.8-in.(71.12 mm) Diameter</p>	 <p>2.8-in.(71.12 mm) Diameter</p>

Figure 4.3 Plan Views of Specimens in Cases C1 to C4 Showing the Positioning of the Oversized Particles at Each Level of Specimens

Additionally, all specimens have few fines (% passing #200 sieve < 1 %) so that this investigation concentrates on the effect of oversized particles as well as their positioning with the specimen without adding the fines content.

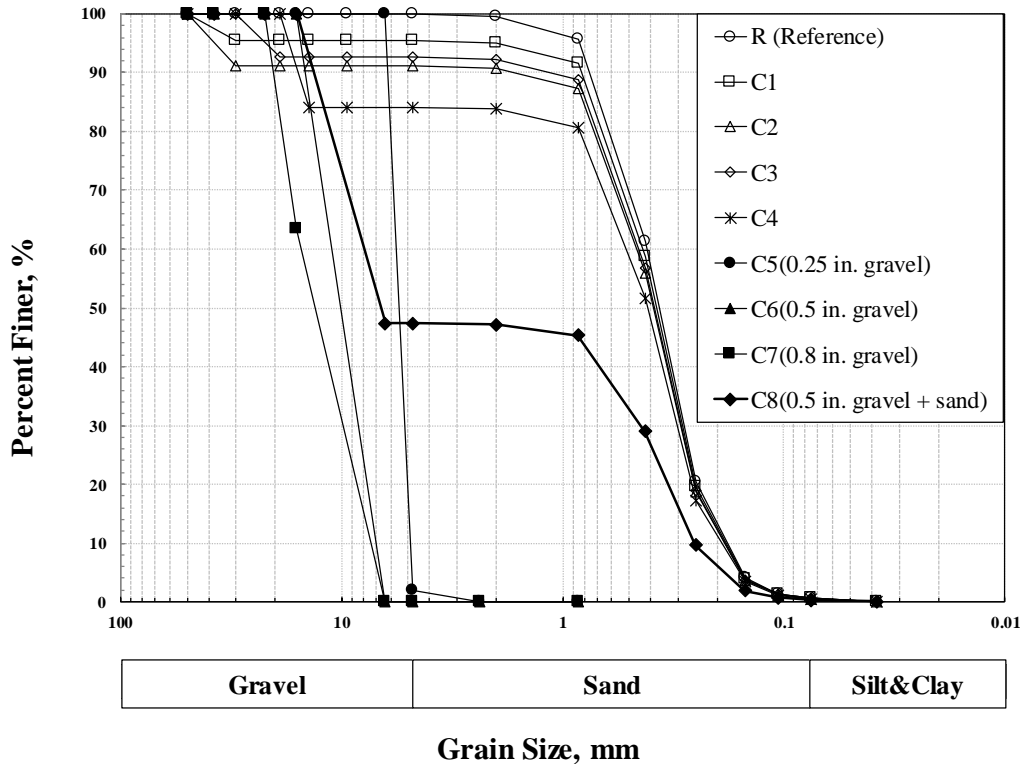


Figure 4.4 Grain Size Distribution of Specimens of Cases C1 through C8 and Uniform Reference Sand

Specimen properties in terms of unit weights, void ratios and so on, are presented in Table 4.3 (a) and 4.3 (b). As seen, all specimens for Cases C1 through C4 have quite similar dry unit weights and initial void ratios. Dry unit weights ranged from 104.8 to 109.8 lb/ft³, and initial void ratios ranged from 0.51 to 0.58. For the uniform gravel specimens

(C5 through C7), no large differences occurred for the dry unit weights and initial void ratios which ranged from 94.8 to 103.0 lb/ft³ and 0.56 to 0.68, respectively. The specimen with the most unusual gradation curve was C8. This specimen was approximately half gravel and half sand. Specimen C8 had the highest dry unit weight of 135.4 lb/ft³ due to the sand filling the voids in the gravel. Additionally, obtaining the initial void ratio of the sand-gravel mixture was rather difficult and time-consuming, both theoretically and technically. Table 4.3 (a) and 4.3 (b) also show that all specimens were reconstituted with a narrow range in water contents of 7.2 % to 7.9 % for the sandy specimens. The gravelly specimens were reconstituted dry.

In the Table 4.3 (b), the grain size characteristics determined from the gradation curves (Figure 4.4) of each specimen are presented. The median grain size, D_{50} , represents the median diameter of a specimen and is often used to estimate small-strain shear modulus at one atmosphere for sandy and gravelly soils (Menq, 2003). The values of D_{50} for Cases C1 through C4 ranged from 0.38 to 0.42 mm. These values are not quite different from the uniform sand specimen (R). It implies that the sizes and locations of oversized gravel particles do not have a strong relationship with the median grain size. The uniformity coefficient, C_u , is calculated by:

$$C_u = \frac{D_{60}}{D_{10}} \tag{4.1}$$

where D_{60} = diameter corresponding to 60 % finer, and

D_{10} =diameter corresponding to 10 % finer in the particle size distribution curve.

Table 4.3 (a) Specimen Properties

Case ID.	Specimen ID.		Total Unit Weight (pcf)		Dry Unit Weight (pcf)		Initial Void Ratio		Specific Gravity	
	Symmetric	Asymmetric	Sym.	Asym.	Sym.	Asym.	Sym.	Asym.	Sym.	Asym.
Reference	$R_{avg.}$		114.7		106.7		0.55		2.65	
1	C1S	C1A	113.6	115.4	104.8	106.7	0.58	0.55	2.65	2.65
2	C2S	C2A	115.4	119.8	104.8	109.8	0.57	0.51	2.65	2.65
3	C3S	C3A	116.7	111.1	107.3	105.5	0.54	0.57	2.65	2.65
4	C4S	C4A	117.3	114.2	108.0	104.8	0.53	0.58	2.65	2.65
5	C5 (1/4" Gravel)		99.8		99.8		0.59		2.53	
6	C6 (1/2" Gravel)		103.0		103.0		0.56		2.56	
7	C7 (1" Gravel)		94.8		94.8		0.68		2.57	
8	C8 (1/2" Gravel + Sand)		135.4		135.4		-		-	

Table 4.3 (b) Specimen Properties

Case ID.	Degree of Saturation (%)		Water Content (%)		Degree of Saturation		Water Content		Grain Characteristics			USCS
	Sym.	Asym.	Sym.	Asym.	(%)	(%)	(%)	(%)	D_{50} , mm.	C_u	C_c	
Reference	37		7.5		0		0.0		0.37	2.27	1.05	SP
1	34	37	7.2	7.5	34	37	7.2	7.5	0.38	2.38	1.01	SP
2	37	41	7.5	7.4	37	41	7.5	7.4	0.39	2.49	0.98	SP
3	38	34	7.6	7.7	38	36	7.6	7.5	0.39	2.45	1.01	SP
4	39	37	7.5	7.9	39	37	7.5	7.9	0.42	2.68	0.92	SP
5	0		0.0		0		0.0		5.50	1.14	0.95	GP
6	0		0.0		0		0.0		10.00	1.46	1.01	GP
7	0		0.0		0		0.0		14.00	1.43	1.25	GP
8	0		0.0		0		0.0		6.80	32.00	0.10	-

This parameter is a useful grain size characteristic of estimating the sensitivity to confining pressure change (Menq, 2003). The Specimen C8 has the highest C_u value of 32.00 and the other specimens have the values in the narrow range of 1.14 to 2.49.

A summary of the total weights and volumes of the oversized particles for Cases C1 to C4 is given in Table 4.4. For example, Case C2 had gavel particles G1 and G2 placed in the specimens. These two particles had a total weight and a total volume, 75.89 g and 29.0 cm³, respectively. These values for Case C2 were normalized by the total weight and total volume of the single particle in Case C1 of 36.43 g and 14.00 cm³, respectively. The comparison of the total weights and total volumes of gravel particle for Case C2 and for the other cases are presented in Table 4.4. In conclusion, Case C2 had about two times for weight and volume of gravel particles compared with C1. Cases C3 and C4 had almost 20% different weights and volumes of gravel particles compared to Case C1. Additionally, portion of the oversized particles for the cases are presented.

Table 4.4 Comparison of the Weights and Volumes of Gravels for Cases C1 to C4

Case ID.	Weight of Gravel Particles, g	Volume of Gravel Particles, cm ³	Normalized Weight of Gravel by Case 1	Normalized Volume of Gravel by Case 1	Portion of Gravel in Weight, %	Portion of Gravel in Volume, %
C1	36.43	14.00	1.00	1.00	3.3	2.3
C2	75.89	29.00	2.08	2.07	6.8	4.8
C3	29.08	11.10	0.80	0.79	2.6	1.9
C4	44.91	17.50	1.23	1.25	4.0	3.0

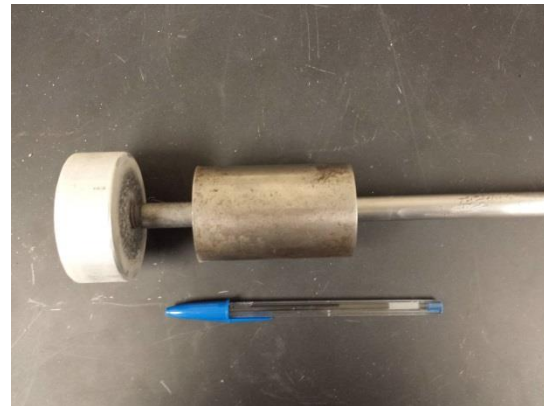
4.4 SPECIMEN PREPARATION AND TESTING PROGRAM

4.4.1 Preparation of Specimens: Undercompaction Method

Each specimen was reconstituted as a right-cylindrical specimen with the diameter of 2.8 inches and the height of 5.6 inches. The undercompaction method (Ladd, 1978) was used. The specimens were compacted with 5 lifts in which the target height of each lift was pre-calculated. A split stainless steel mold of about 2.8 inches inner diameter and a 2-lb drop hammer were used to reconstitute the specimens. The mold and drop hammer are shown in Figure 4.5. An attempt was made to compact the reconstituted specimen to the same water content so that it keeps the property from playing a role in these comparison tests.



(a) Split Compaction Mold



(b) Compaction Drop

Figure 4.5 2.8 inch Compaction Mold and Compaction Hammer

The compaction hammer is composed of an aluminum bottom plate, a stainless steel hammer, and a moving-guide rod. Because the hammer falls only through the bar up to the bottom plate, the energy of the falling hammer is delivered directly to the specimen through the plate. The bottom compaction but also protect membranes from puncturing.

4.4.2 Test Programs

The dynamic properties of the soil specimens tested in this study were performed both in the linear ($\gamma < 10^{-3}$ %), as called “low amplitude” resonant column testing (RC-LAT), and in the nonlinear range ($\gamma > 10^{-3}$ %), as called “high amplitude” resonant column testing (RC-HAT).

Staged confinement was used in this study. The stage loading consisted of five confining-pressure levels. This staging was used to determine how the effects of oversized particles changed the dynamic properties for each specimen compared to sand-only specimens. The testing schedule is given in Table 4.5. RC-LAT tests lasted for about 60 minutes at each pressure to determine any time effect on the dynamic properties at the pressure levels. Typically, the pressure level schedule is related to the estimated in-situ mean effective confining pressures and includes confining pressure at $\frac{1}{4}$, $\frac{1}{2}$, 1, 2, and 4 times the estimated in-situ pressures. However, because specimens in this study were not intact specimens recovered from a field site, a representative field confining pressure of 18 psi for these specimens was selected. Based on the estimated mean effective stress (18 psi), the other pressure levels were determined and shown in the Table 4.5. Discrete data points

were collected throughout the duration of low-amplitude RC testing. In this way, any effect of time under confinement should be determined.

RC-HAT tests were performed both on the third (18 psi) and fifth pressure (72 psi) levels to investigate the nonlinear behavior of the specimens. The high-amplitude tests were performed after the 60 minutes of the confining pressure on the small-strain dynamic properties was completed. This procedure was followed to avoid the impact of stain history on the small-strain dynamic properties. The shear modulus reduction and material damping ratio curves were obtained from the series of RC-HAT tests.

Table 4.5 Testing Schedule for RC Testing of Specimens of Sand and Sand with Gravel Particles

Isotropic Confining Pressure, σ_o , psi					
	4.5	9	18	36	72
RC-LAT	X	X	X	X	X
RC-HAT			X		X

4.5 SUMMARY

The properties of 13 sandy and gravelly specimens were discussed in this chapter. A uniform sand was characterized as called “Reference”. The 8 specimens in Cases 1 through 4 were reconstituted with the uniform sand and 14 oversized gravel particles. The details about the gravel particles and associated with each case were discussed. Additionally, three uniform gravel specimens with different particle size and a unique

mixture of uniform sand and uniform gravel were also reconstituted and tested. Grain-size distribution tests were performed and the accompanying parameters were characterized for each specimen. Lastly, a testing program composed of a series of low-amplitude and high-amplitude resonant column tests were performed.

CHAPTER FIVE

EFFECTS OF OVERSIZED PARTICLES ON SMALL-STRAIN DYNAMIC PROPERTIES

5.1 INTRODUCTION

Before exploring the effects of oversized particles on the small-strain dynamic properties, the dynamic properties of the uniform reference material, the washed mortar sand, are discussed in Section 5.2. The effects of oversized particles on small-strain shear modulus is then presented in Section 5.3. The effects of the oversized particles on small-strain material damping ratio is presented in Section 5.4. Finally, the effects of material type on small-strain dynamic properties and an overall summary are presented in Section 5.5 and 5.6, respectively.

5.2 UNIFORM REFERENCE SAND

5.2.1 Small-Strain Shear Modulus

To observe and recognize the effect of oversized particles on the dynamic properties, it is necessary to first investigate the dynamic properties of the uniform sand without any oversized particles. Therefore, the three uniform reference sand specimens were reconstituted with the reference washed mortar sand described previously in Chapter 4 and tested in the RCTS device. In this section, the small-strain shear moduli of the three different uniform sand specimens (R_1, R_2, and R_3) are examined and a reference range in moduli consisting of the results of those specimens is generated.

As described, the specimens R_1, R_2, and R_3 are uniform sand specimens reconstituted with washed mortar sand. The three specimens were targeted as similar as possible in terms of dimensions, water content, and dry density. This three specimens are nearly identical with dry unit weight, water content and initial void ratio all with about $\pm 3\%$ of each other. To examine the variability of measurements of the small-strain shear modulus, the RCTS testing performed on specimen R_1, R_2, and R_3, are presented in the Figures 5.1 (a), (b), and (c), respectively.

To compare the test results, a power law expression (Equation 2.4) was fit to each data set and the numerical coefficients were used to compare quantitatively the degree of stiffness and sensitivity to confining pressure. In this expression, the parameters, A_G and n_G represent the small-strain shear modulus at a confining pressure of 1 atm (14.7 psi) and the exponent of the confining pressure term in the relationship, respectively. The least squares regression method was also used to provide best-fit lines based on the measurements.

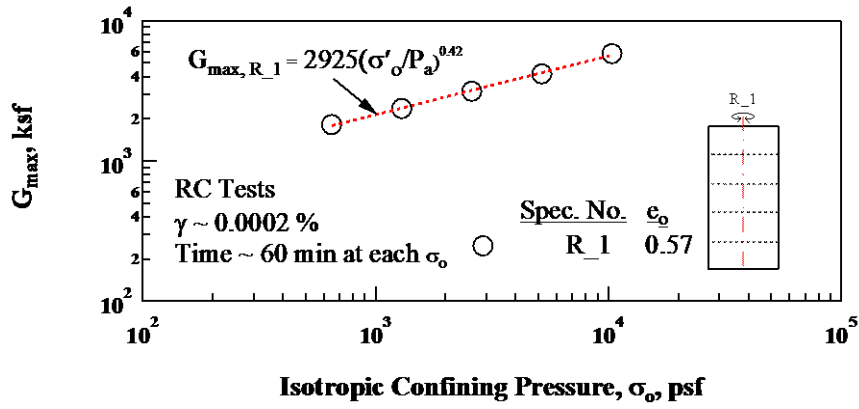
As seen, the three uniform sands exhibit varying values of n_G , ranging from 0.42 to 0.48 and also varying values of A_G from 2925 to 3358 ksf. It is valuable to notice that the value of A_G for Specimen R_3 is the highest value and this specimen has the lowest initial void ratio, 0.53. The same is true for the Specimen R_1 which has the lowest A_G and the highest void ratio. This relationship follows the reciprocal relationship of the small-strain shear modulus at 1 atm with the initial void ratio as first proposed by Hardin and Black (1968). Additionally, the values of n_G do not seem to be strongly related to the initial void ratio of the specimens with this parameter best correlated with the uniformity coefficient, C_u of granular material (Menq, 2003). In any case, the values of the parameters are generally within about $\pm 10\%$ of the average.

Comparison of the $\log G_{\max} - \log \sigma_o$ relationships for the three specimens is shown in Figure 5.2. This comparison allows a reference range in the $\log G_{\max} - \log \sigma_o$ relationship to be determined and shows the general variability created by specimen construction. This reference range is placed on the back layer of every figure in the next section to represent a control range of variability for which no effect can be contributed to oversized particles.

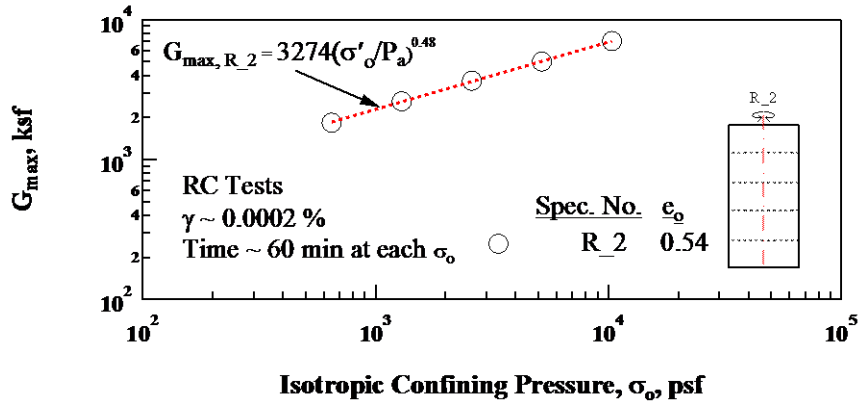
In conclusion, the variability due to specimen construction in terms of the $\log G_{\max} - \log \sigma_o$ relationship is not very significant, as expected. And it is reasonable to use this variability as a gage of the variability due to specimen construction on the small-strain shear modulus.

5.2.2 Small-Strain Material Damping Ratio

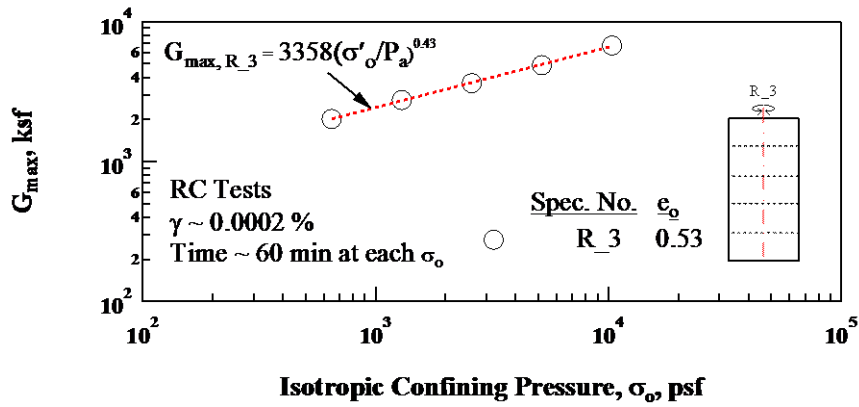
Variations of small-strain material damping ratio with isotropic confining pressure for the three uniform sand specimens are shown in Figure 5.3. The power law expression (Equation 2.6) was used to compare quantitatively the degree of energy dissipation at varying confinements and sensitivity of the confining pressure change. The parameters in the power law expression are A_D and n_D , which are the small-strain material damping ratio at a confining pressure of 1 atm (14.7 psi) and the exponent of effective confining pressure in the relationship, respectively.



(a) Uniform Specimen R_1



(b) Uniform Specimen R_2



(c) Uniform Specimen R_3

Figure 5.1 Comparison of the Variations of Low-amplitude Shear Modulus with Isotropic Confining Pressure from Resonant Column Tests of Uniform Sand Specimens R_1, R_2, and R_3

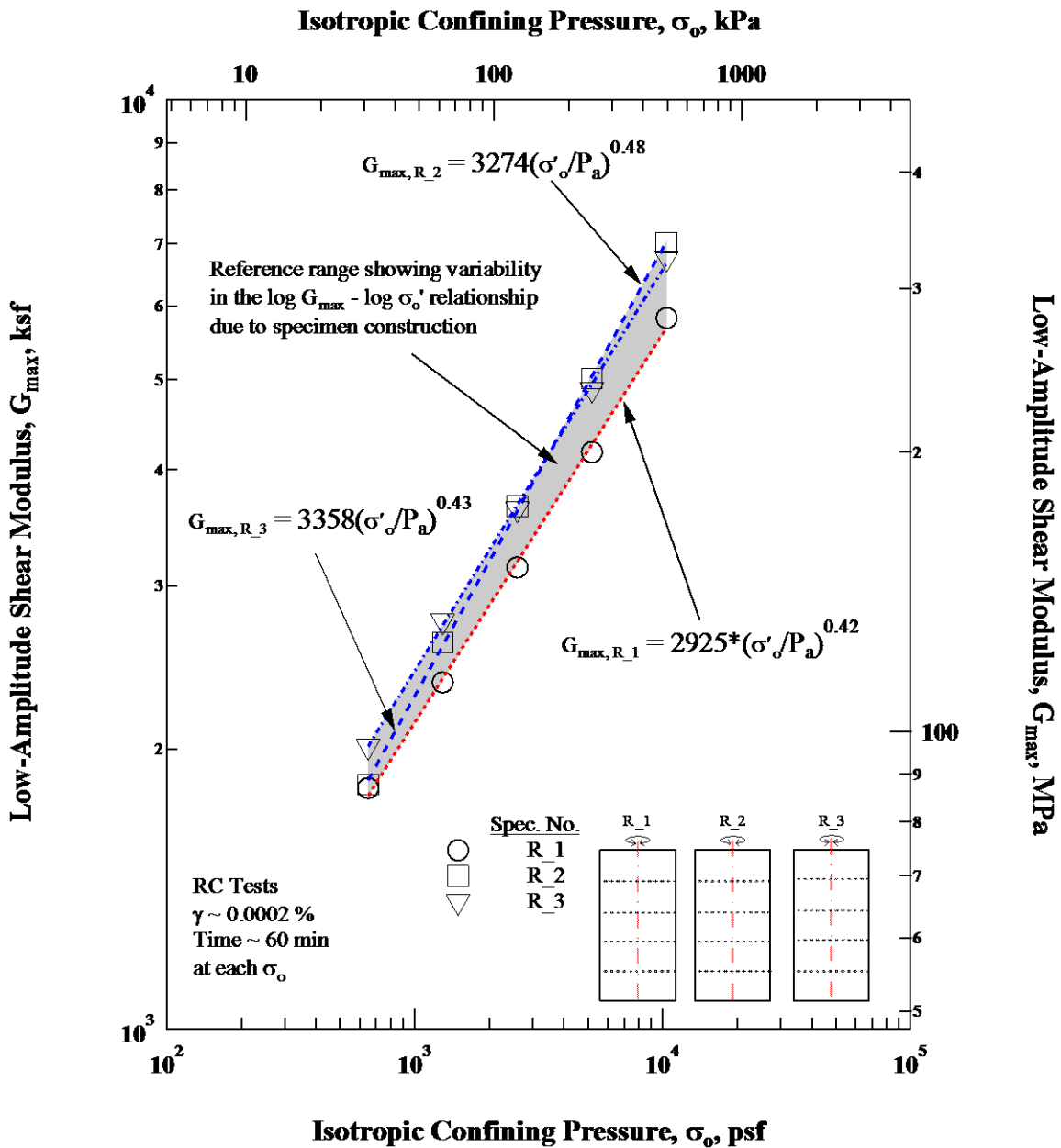
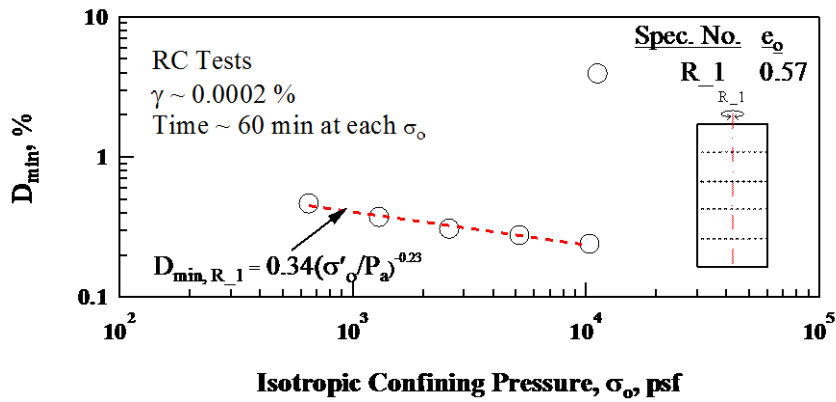


Figure 5.2 Comparison of the Variation of Low-Amplitude Shear Modulus with Isotropic Confining Pressure from Resonant Column Tests of Uniform Sand Specimens R_1, R_2, and R_3

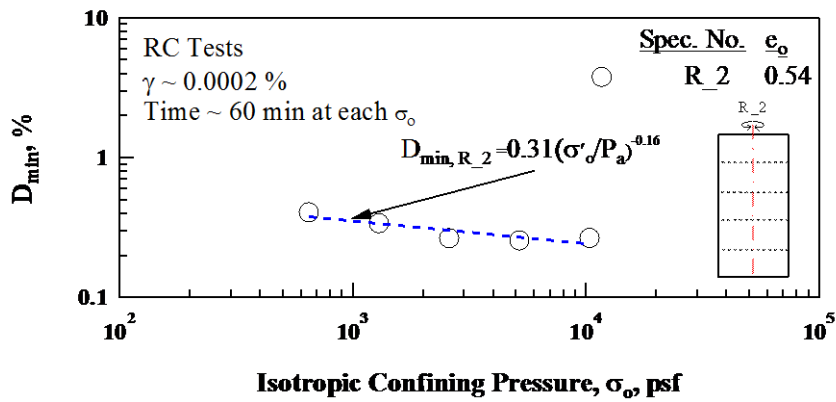
As seen in Figure 5.3, the three uniform sand Specimens of R_1, R_2, and R_3 exhibit varying values of n_D , ranging from -0.16 to -0.23 and also the value of A_D from 0.31 to 0.34. Unlike the case of $\log G_{\max} - \log \sigma_o$ relationship, there seems to be no correlation between the values of A_D and the initial void ratio, e_o . This relationship is different from the approximate estimation by Laird (1994) that D_{\min} values generally at a confining pressure of 1 atm in proportional to the initial void ratio, e_o . In addition, the measurement of material damping ratio is much more sensitive than G_{\max} to other factors such as equipment-generated damping and background noise. Also D_{\min} is not very sensitive to material density. Menq (2003) also mentioned that there was little correlation between grain distribution characteristics and small-strain material damping ratio, D_{\min} , outside factors that make material damping ratio measurements much more difficult than G_{\max} measurements.

Comparison of the $\log D_{\min} - \log \sigma_o$ relationships for the three sand specimens are presented in Figure 5.4. This comparison allows a reference range of the trend lines from the measurements of the D_{\min} be determined. This range indicates the variability due to specimen construction in the $\log D_{\min} - \log \sigma_o$ relationships. This control range is then used just like the G_{\max} control range to represent a range of variability which cannot be attributed to oversized particles.

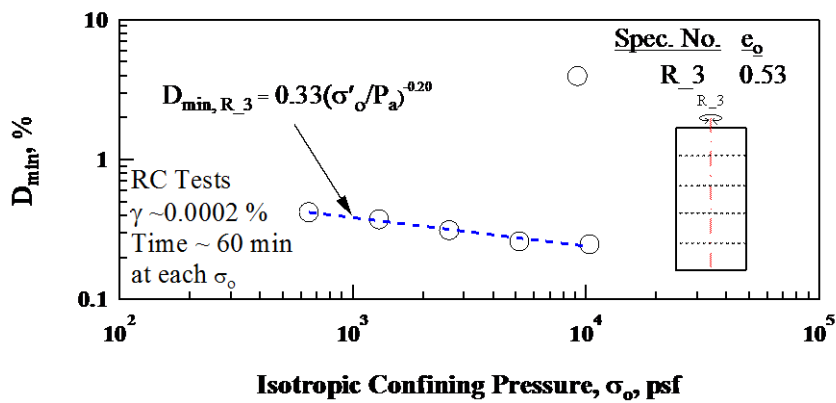
In conclusion, the variability in terms of the $\log D_{\min} - \log \sigma_o$ relationship does not seem to be significant, as expected. This finding is reasonable and gives some variability due to a specimen construction. As with G_{\max} , determination of the reference range is used with a gray zone on the back layer of all figures in the next section.



(a) Uniform Specimen R_1



(b) Uniform Specimen R_2



(c) Uniform Specimen R_3

Figure 5.3 Comparison of the Variations of Low-Amplitude Material Damping Ratio with Isotropic Confining Pressure from Resonant Column Tests of Uniform Sand Specimens R_1, R_2, and R_3

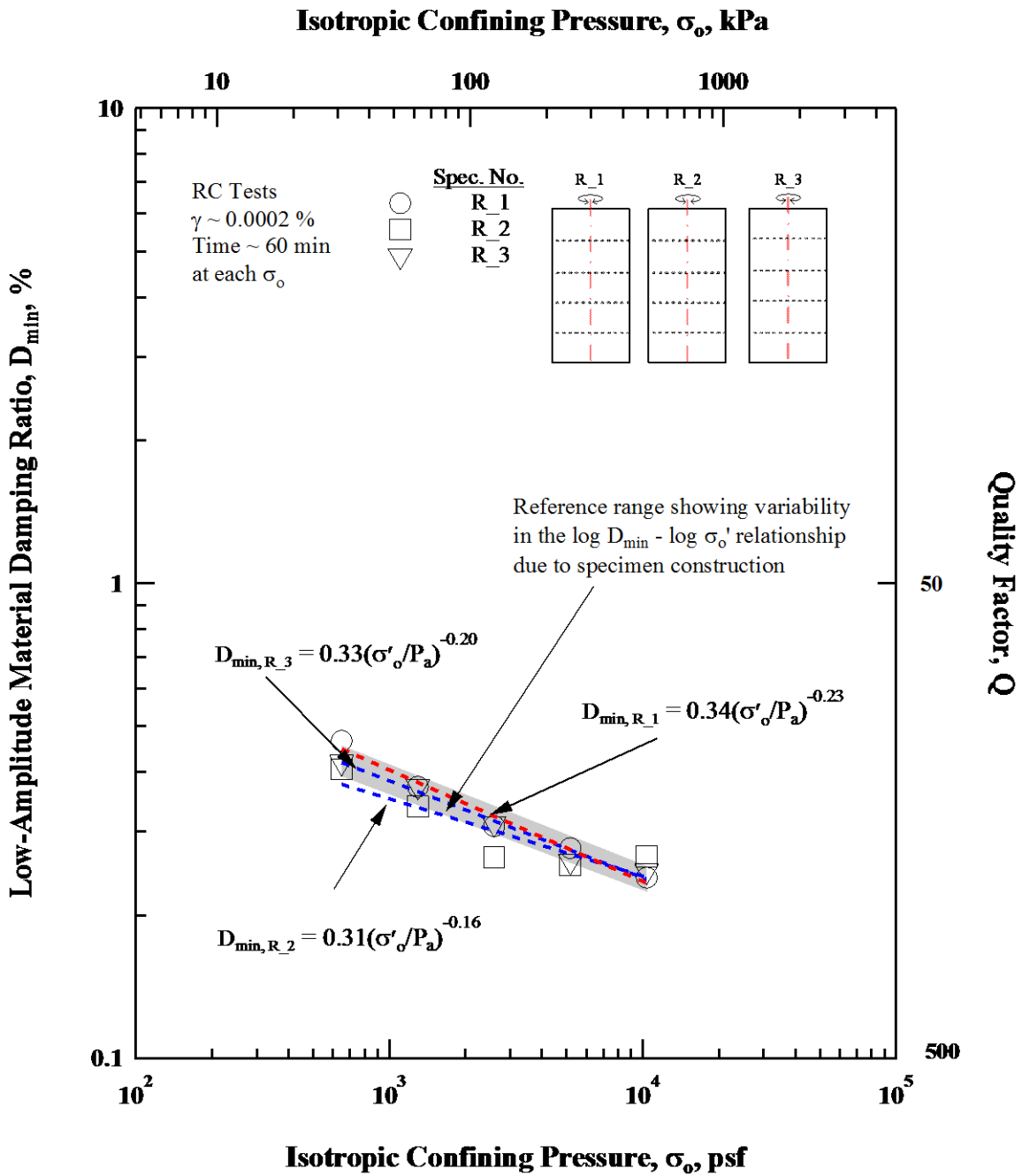


Figure 5.4 Comparison of the Variation of Low-Amplitude Material Damping Ratio with Isotropic Confining Pressure from Resonant Column Tests of Uniform Sand Specimens R_1, R_2, and R_3

5.3 EFFECTS ON SMALL-STRAIN SHEAR MODULUS OF OVERSIZED PARTICLES

5.3.1 Largest Oversized Particles

As described in the previous chapter, all gravel particles in this study were divided into three groups; (1) “largest” particles of G1 and G2, (2) “relatively larger” particles of G3 through G5, and (3) “large” particles of G6 through G14. In this section, the effects of the largest particles (G1 and the combination of G1 and G2) on the small-strain shear modulus are discussed.

The effects of the “largest” oversized particle (G1) located both at the longitudinal axis of the specimen (C1S, which is the symmetric specimen) and outside of the longitudinal axis (C1A, which is the asymmetric specimen) on the small-strain shear modulus at varying confining pressures are presented in Figure 5.5. Also the gray zone in the figure represents the reference range of the uniform sand specimens in Figure 5.2. At the relatively low pressure levels, which are about 4 psi to 18 psi, Specimens C1S and C1A exhibit a slightly overconsolidated portion (OC). The OC zone was likely caused during the reconstitution of the specimens. The target relative density for all specimens was over 95 %, and the values achieved were all over 94 %. Therefore, to compare the dynamic parameters, only on the NC portions, which are relatively at high pressures from about 18 psi to 72 psi, are used. This range was selected to eliminate the possibility that reconstitution variability in the OC portions might overly influence the study.

In Figure 5.5, the symmetric Specimen C1S (the gravel of G1 was on the axis of rotation) is slightly below reference range. On the other hand, asymmetric Specimen (C1A) is slightly above (or nearly at) the shear modulus range of the uniform sand specimens. In other words, the asymmetric specimen is stiffer dynamically than not only the symmetric specimen but also the uniform sand. However, the magnitudes of increase and decrease of

stiffness for the asymmetrical and symmetrical specimens do not seem to be very significant.

One important finding is that the values of G_{\max} for the symmetrical specimen (C1S) are smaller than the asymmetrical specimen (C1A). This result indicates the location of G1 could affect the stiffness of specimen (A_G), especially for specimens that become stiffer when the largest particle is offset from the central section of the specimen. This finding seems to be important even though there are no significant variations in the critical parameters of median grain size (D_{50}) and initial void ratio (e_0) (Menq, 2003). This finding is examined subsequently for the other cases for which different sizes and numbers of oversized particles are installed in the sand specimen. However, the result seems to be likely due to the fact the symmetrical, central location experiences lower strains and the asymmetrical location experiences higher strains.

Both specimens showed no significant change in the value of n_G , ranging from 0.45 to 0.47. This results indicates that the oversized particle of G1 did not affect the sensitivity to changes in the confining pressure, following the general trend from Menq (2003) that the n_G parameter is primarily affected by uniformity coefficient, C_u . Table 4.3 (b) in Chapter 4 also shows that the oversized particles did not change that parameter (C_u) significantly.

The test results in terms of the $\log G_{\max} - \log \sigma_0$ relationships of the cases that contained the two largest particles (G1 and G2) are presented in Figure 5.6. Both the symmetrical and asymmetrical specimens (C2S and C2A) again showed OC portions.

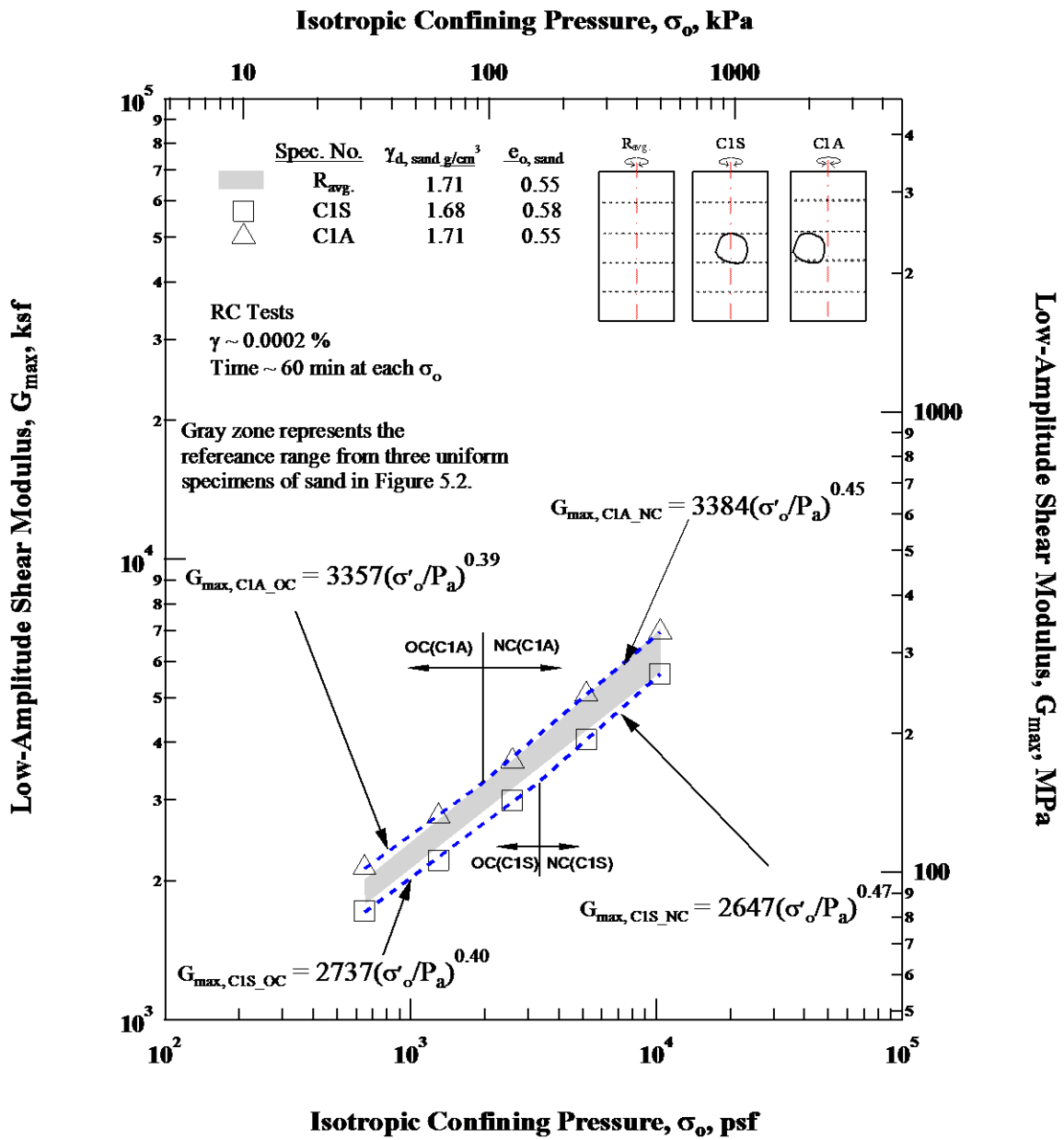


Figure 5.5 Comparison of the Variation of Low-Amplitude Shear Modulus with Isotropic Confining Pressure from Resonant Column Tests of the Three Reference Sand Specimens, and Specimens C1S and C1A with the Largest Gravel Particle

Specimen C2S showed values of G_{\max} of C1S, especially in the comparison of the values of A_G in the NC range, with the difference is less than 1 %. This result seems to indicate that adding the second “largest” particle (G2) at the axis of rotation affected the dynamic shearing stiffness very little. This presumably occurred because the central portion of specimen undergoes very little strain due to rotation.

It is interesting to see that G_{\max} values of Specimen C2S is slightly below the reference range. This slight decrease in stiffness also occurred for Specimen C1S. Even though the values of G_{\max} of Specimen C2A at low pressures (OC portion) are closer to the upper limit of the reference range, and at high pressures (NC portion) the G_{\max} values are within the reference range. In this case, the two “largest” particles had no significant effect on G_{\max} .

However, it again is shown that the values of G_{\max} for the asymmetrical specimen (C2A) are greater than the values of G_{\max} for the symmetrical specimen (C2S) following the finding from Specimens C1S and C1A.

Conclusively, the “largest” particles did not significantly affect the stiffness of the uniform sand. However, the asymmetrical property inside the specimens consistently increased the stiffness of the uniform sand slightly and were always stiffer than the specimens with symmetrically located oversized particles.

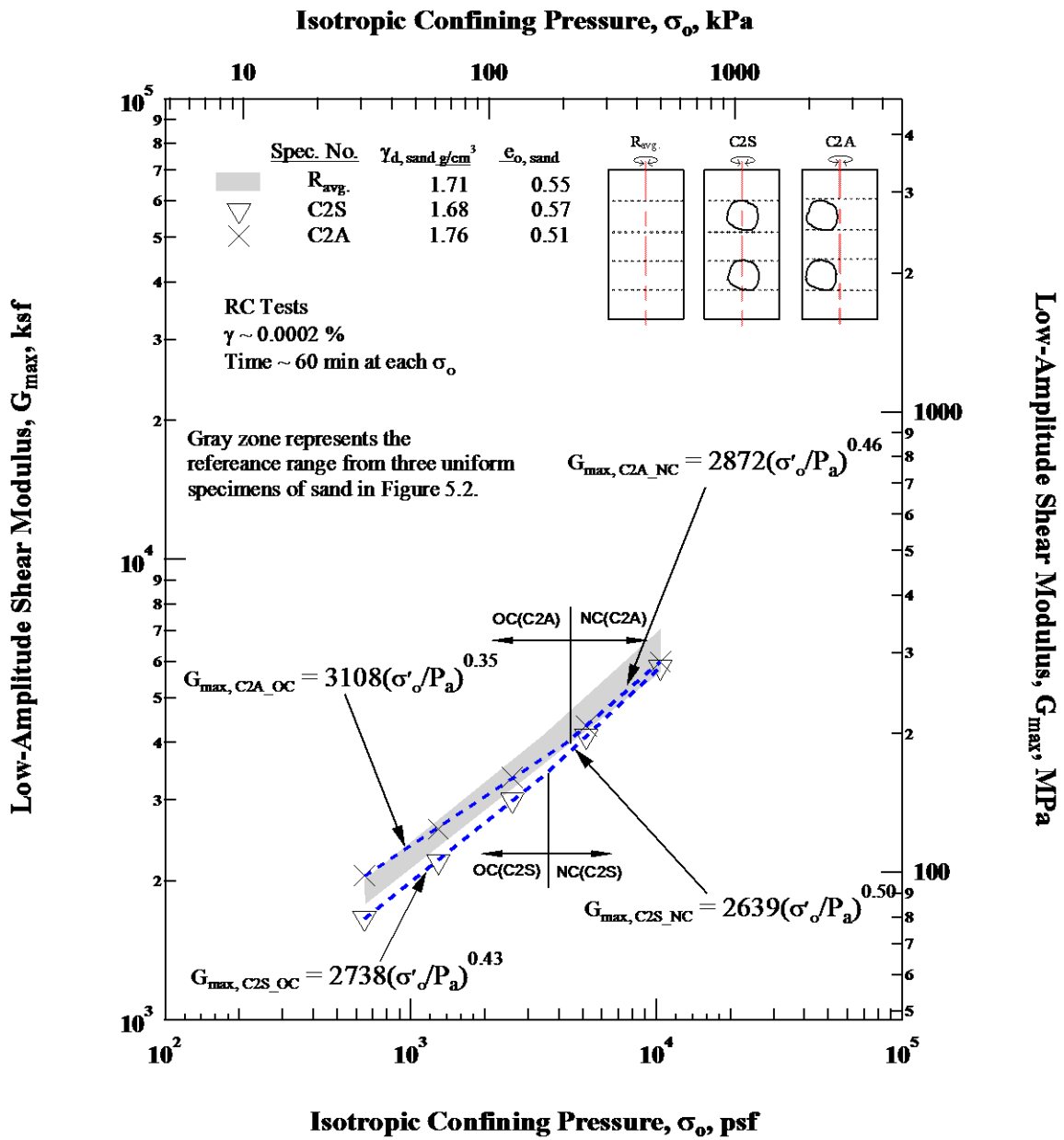


Figure 5.6 Comparison of the Variations of Low-Amplitude Shear Modulus with Isotropic Confining Pressure from Resonant Column Tests of the Three Reference Sand Specimens, and Specimens C2S and C2A with the Largest Gravel Particles

5.3.2 Relatively Larger and Large Oversized Particles

In this section, the effects of the “relatively larger” particles (G3 to G5) and the “large” particles (G6 to G14) on the $\log G_{\max} - \log \sigma_o$ relationships are presented. As described in Chapter 4, the oversized particles of G3 to G5 have the average diameter of about 0.8 inches and are classified in this study as “relatively larger” particles, while the diameters of G1 and G2 are larger than 1 inches (1.3 inches) and are classified as the “largest” particles. However, the three larger particles in Specimen C3S are gathered at the axis of rotation in the middle layer of the specimen, so that the equivalent diameter of the particles could be considered comparable to Specimen C1S. As a result, the equivalent diameter of G3 to G5 is about 1.8 inches, which is about 35 % larger than the G1 or G2, but it is still less than half of the specimen diameter.

The effects of “relatively large” particles (G3 to G5) on the $\log G_{\max} - \log \sigma_o$ relationships for the Specimens C3S and C3A are presented in Figure 5.7. The C3S do not exhibit an OC portion, indicating no over compaction specimen during construction. For low pressure levels, including a mean effective stress of 18 psi, values of G_{\max} for both specimens were generally below the range of the gray zone for the uniform reference sand, meaning a reduction in the small-strain shear modulus compared to the uniform sand. Above these pressures, the two specimens showed values of G_{\max} within the range of the uniform reference sand.

It is again interesting to focus on the values of A_G for Specimens C3S and C3A. The value of 2649 ksf for Specimen C3S is almost same as value of 2647 ksf for Specimen C1S. This result indicates that the size or aggregation of oversized particles

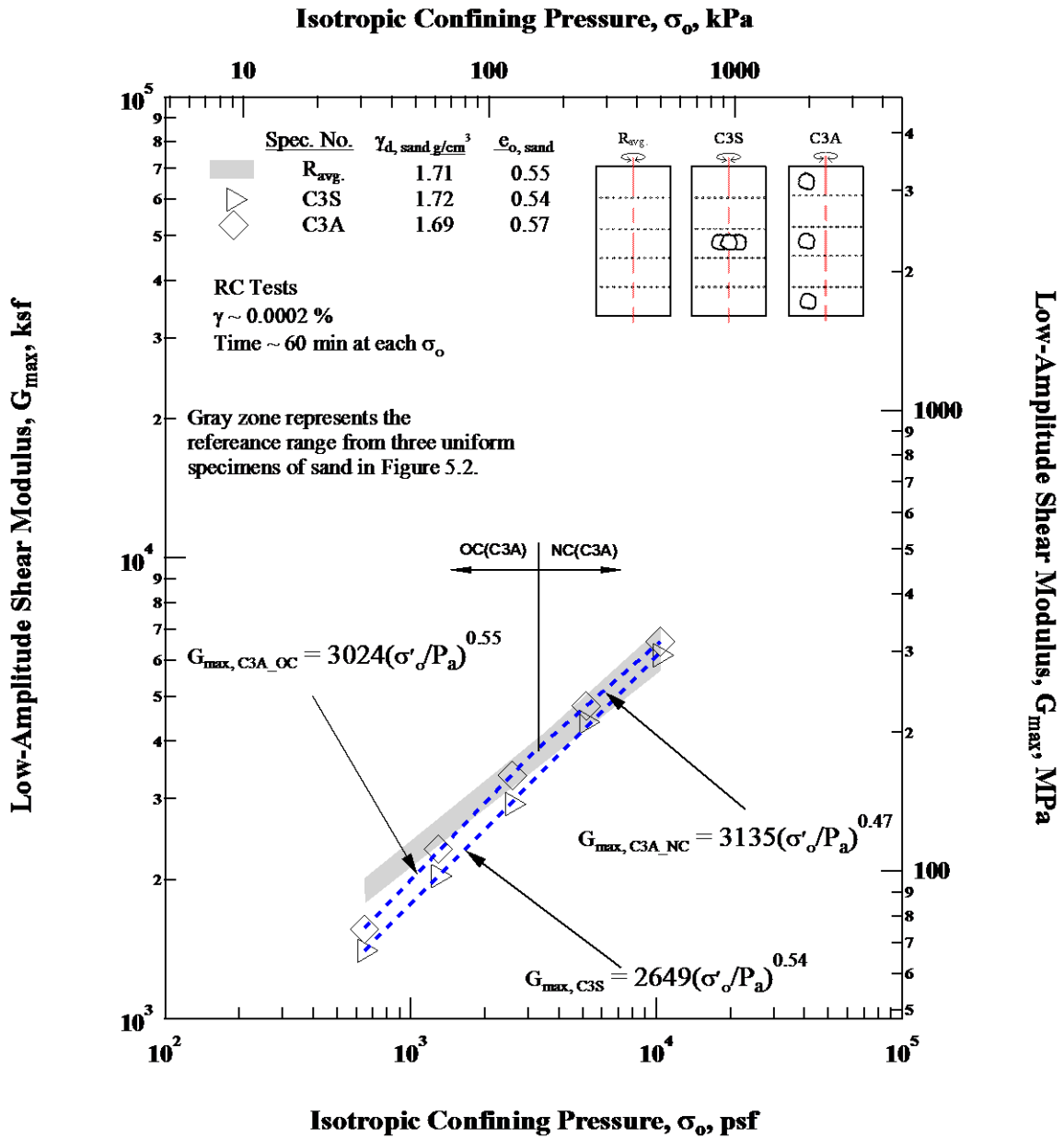


Figure 5.7 Comparison of the Variation of Low-Amplitude Shear Modulus with Isotropic Confining Pressure from Resonant Column Tests of the Three Uniform Sand Specimens and C3S and C3A with the Relatively Larger Gravel Particles

affect the stiffness of the sand very little as long as the oversized particles are located along the axis of rotation. Another key point is that, once again the G_{\max} values of asymmetrical Specimen C3A are greater than Specimen C3S. This finding is agreement with the result for cases of C1 and C2 with the largest particles. A comprehensive explanation needs further study but it does seem the oversized particles near the outside edge of the specimen stiffer the specimen.

Comparisons of the $\log G_{\max} - \log \sigma_o$ relationships for specimens that were reconstituted with the “large” particles (G6 through G14) are presented in Figure 5.8. The average diameter of these particles is about 0.6 inches and the equivalent diameter of three particles of G6, G7 and G8 (or G9, G10 and G11 or G12, G13 and G14) is about 1.4 inches. This equivalent diameter is about 7 % larger than G1 or G2 and about 21 % smaller than the equivalent diameter of G3, G4 and G5.

Specimen C4S had the values of G_{\max} that were generally below the range of gray zone until about the pressure of 36 psi (5184 psf). The reduction in small-strain modulus compared to the uniform sand appeared around 18 psi (2582 psf) for asymmetrical Specimen C4A. Above these pressures, this two specimens showed values of G_{\max} within the range of the uniform reference sand.

One difference from the general trend is that the increase of the G_{\max} values for asymmetrical specimen did not occurred in this case. Above the pressure of about 14 psi (2016 psf), the $\log G_{\max} - \log \sigma_o$ relationships of two specimens are almost identical. On the other hand, below the pressure (about 14 psi), the symmetrical Specimen C4S rather had higher G_{\max} values. It indicates that the effect of the “large” oversized particles located near the outside edge of the specimen is less than the other cases.

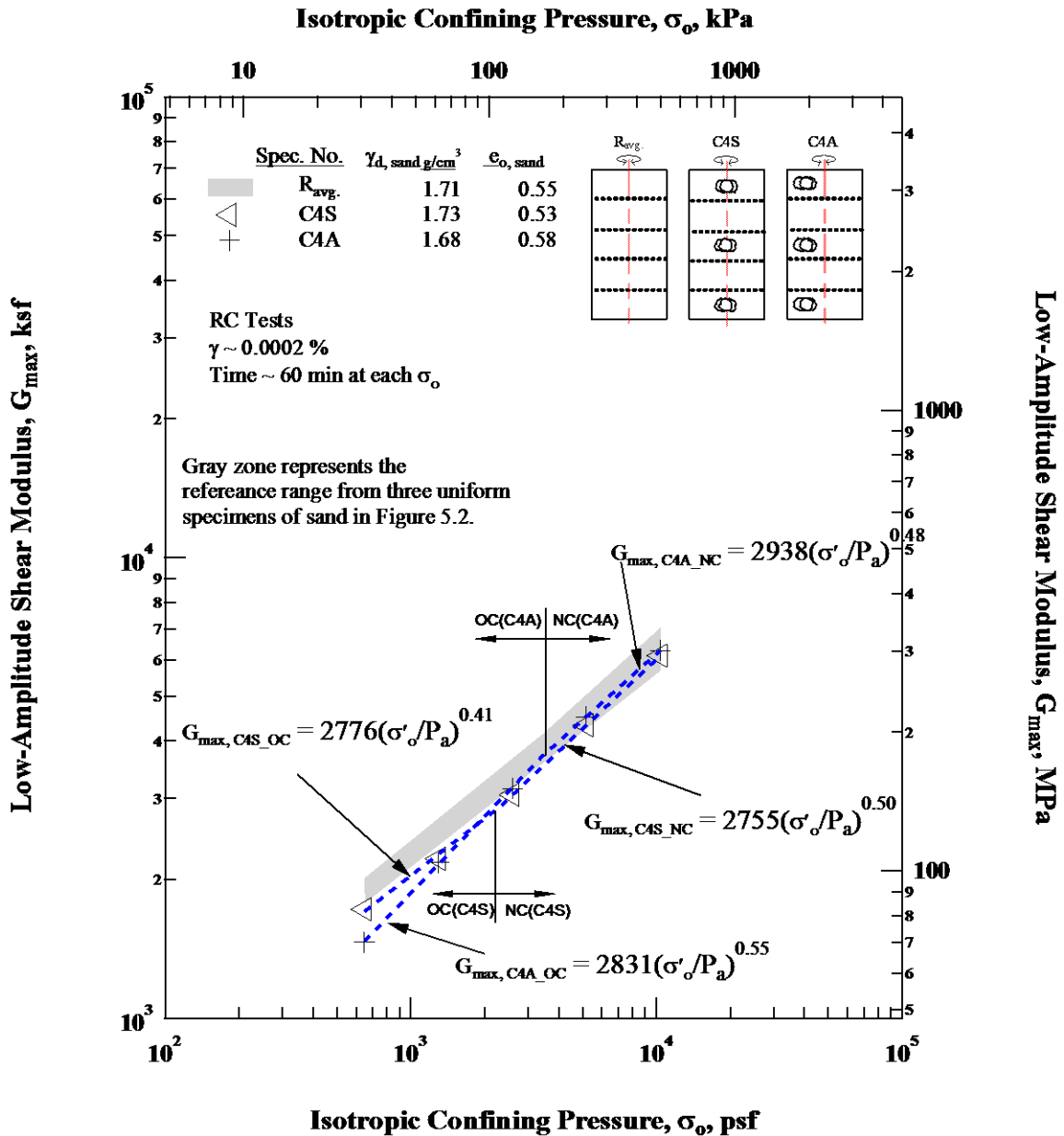


Figure 5.8 Comparison of the Variation of Low-Amplitude Shear Modulus with Isotropic Confining Pressure from Resonant Column Tests of the Three Uniform Sand Specimens C4S and C4A with the Large Gravel Particle

5.4 SMALL STRAIN MATERIAL DAMPING RATIO

5.4.1 Largest Oversized Particles

The measurements of the variation of small-strain material damping ratio with isotropic confining pressure were also performed for all specimens containing the oversized particles. Just as with the $\log G_{\max} - \log \sigma_o$ reference range for the uniform sand, a reference range for the $\log D_{\min} - \log \sigma_o$ relationships for uniform sand was created as a gray zone to compare with the results from the oversized particles. This gray reference zone shows the variability of material damping ratio at small strains for the uniform sand and is a very important reference. Additionally, the overconsolidated portions (OC) of the $\log D_{\min} - \log \sigma_o$ relationships were not considered in this study of D_{\min} because the values of D_{\min} were somewhat scattered in the $\log D_{\min} - \log \sigma_o$ relationships due to the increased complexities in performing damping measurements compared to the measurements of G_{\max} .

The effect of the “largest” particle (G1) on the $\log D_{\min} - \log \sigma_o$ relationships of Specimens C1S and C1A is shown in Figure 5.9. Specimen C1S showed little change in terms of the $\log D_{\min} - \log \sigma_o$ relationship compared with the uniform sand. In terms of the comparison of D_{\min} at 1 atm. (A_D), the value of A_D for Specimen C1S is the same as the average value for the three uniform reference sand specimens. For the parameter, n_G , which shows the effect of confining pressure, again the value for symmetrical specimen was nearly the same as the sand.

On the other hand, the values of D_{\min} of asymmetrical Specimen C1A were greater than Specimen C1S and the reference sand for all pressure levels, indicating that energy dissipation was increased in the case where the “largest” particle was located away from the longitudinal axis of rotation. This finding is not surprising if one thinks in

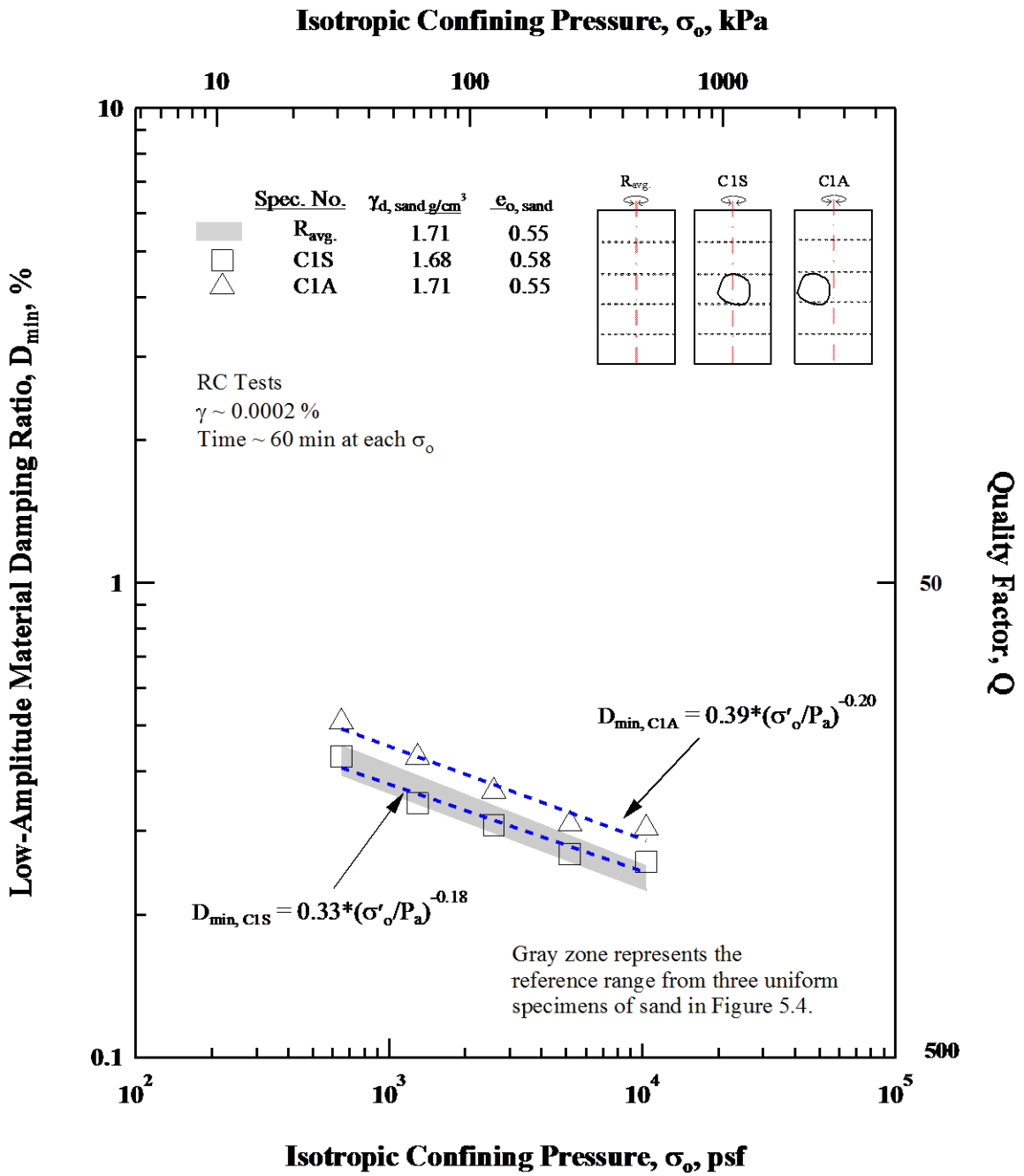


Figure 5.9 Comparison of the Variation of Low-Amplitude Material Damping Ratio with Isotropic Confining Pressure from Resonant Column Tests of Specimens R_{avg.}, C1S, and C1A

terms of larger localized strains occurring around the oversized gravel particle as the particle is offset away from the axis of rotation into a region of higher strains, even though the strains are in the relative small-strain range.

The effect of the combination of the two “largest” oversized particles (G1 and G2) on the $\log D_{\min} - \log \sigma_o$ relationships is presented in Figure 5.10. As expected, any important variation in the $\log D_{\min} - \log \sigma_o$ relationship was not found for either specimen. The A_D of Specimen C2S is 0.33, which is almost same value as the specimens of C1S and R_{avg} . This comparison indicates that no significant energy dissipation would occur from the “largest” oversized particles as long as they are located along the axis of rotation in the specimens.

On the other hand, the Specimen C2A for which the oversized particles of G1 and G2 were installed asymmetrically in the specimen showed a slight increase in the values of D_{\min} at relatively low confining pressures. The finding follows the comparison between C1S and C1A. It is worth mentioning that the material damping ratio at small strains seems to depend on the location of the oversized particles rather than the numbers or sizes of the particles (within the scope of this property). Asymmetrical located the oversized particles could play an important role in the increase of energy dissipation in the small strain range.

In conclusion, there are two key findings in this section which are: (1) there was no effect of the “largest” particle when symmetrically located in the uniform sand, and (2) an increase in small-strain material damping ratio occurred in the asymmetrical Specimen C2A.

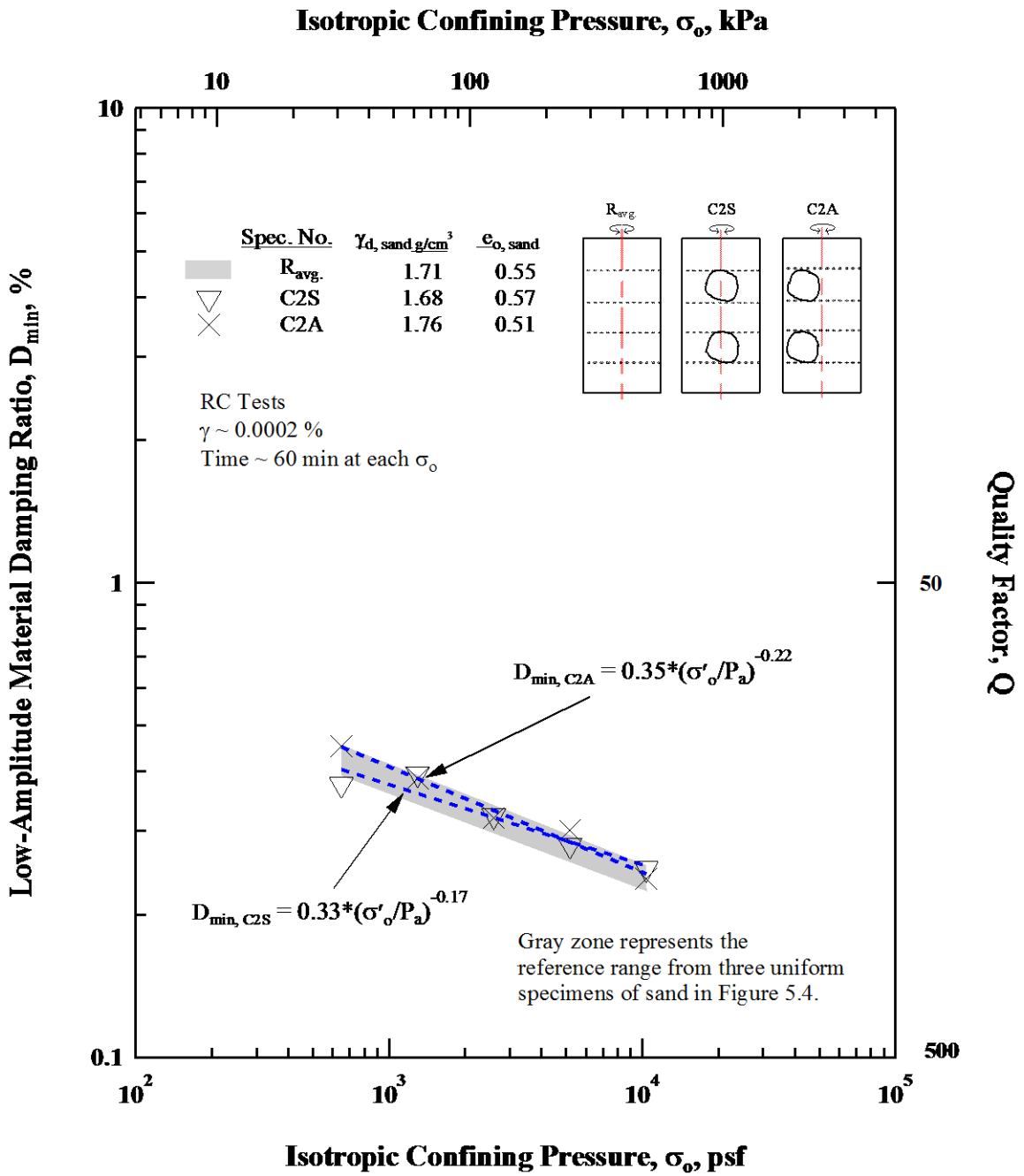


Figure 5.10 Comparison of the Variation of Low-Amplitude Material Damping Ratio with Isotropic Confining Pressure from Resonant Column Tests of Specimens R_{avg} , C2S, and C2A

5.4.2 Relatively Larger and Large Oversized Particles

Comparisons of the variation of D_{\min} with confining pressures of Specimens C3S and C3A are presented in Figure 5.11. As described in the previous chapter (Chapter 4), Specimens C3S and C3A are the specimens for which “relatively larger” particles of G3 through G5 were installed at the axis of rotation and outside the axis of rotation in the specimens, respectively. In this case, it is interesting to observe that the values of D_{\min} for Specimen C3S increased significantly compared to the uniform reference sand as well in comparison to Specimens C1 and C2, even if this specimen has the oversized particles located symmetrically. Contrary to the trend found with the largest particles, the “larger” particles affected D_{\min} more. This strong effect presumably occurred because the equivalent diameter of the three “larger” particles (G3 to G5) is larger than that of the “largest” particles (G1 or G2), thus the aggregate larger contact area allows more energy dissipation between particles in the specimen. In terms of A_G values, the value for Specimen C3S is higher than that of the reference sand, which is about 25% higher material damping ratio. In terms of n_G , Specimen C3S exhibits a steeper (negative) slope relative to the uniform sand.

In terms of the symmetrical or asymmetrical location of the oversized particles, there was more energy dissipated in the asymmetrical specimen, as expected. The explanation for this general trend deserves further study. For Specimen C4S, which has “large” particles (G6 through G14) in the top, middle, and bottom layers in the specimen centered about the axis of rotation, greater material damping occurred in this specimen than the uniform sand. This increase in D_{\min} seems to be significant until the highest pressures. In terms of values of n_G , the asymmetrical specimen was more sensitive to the

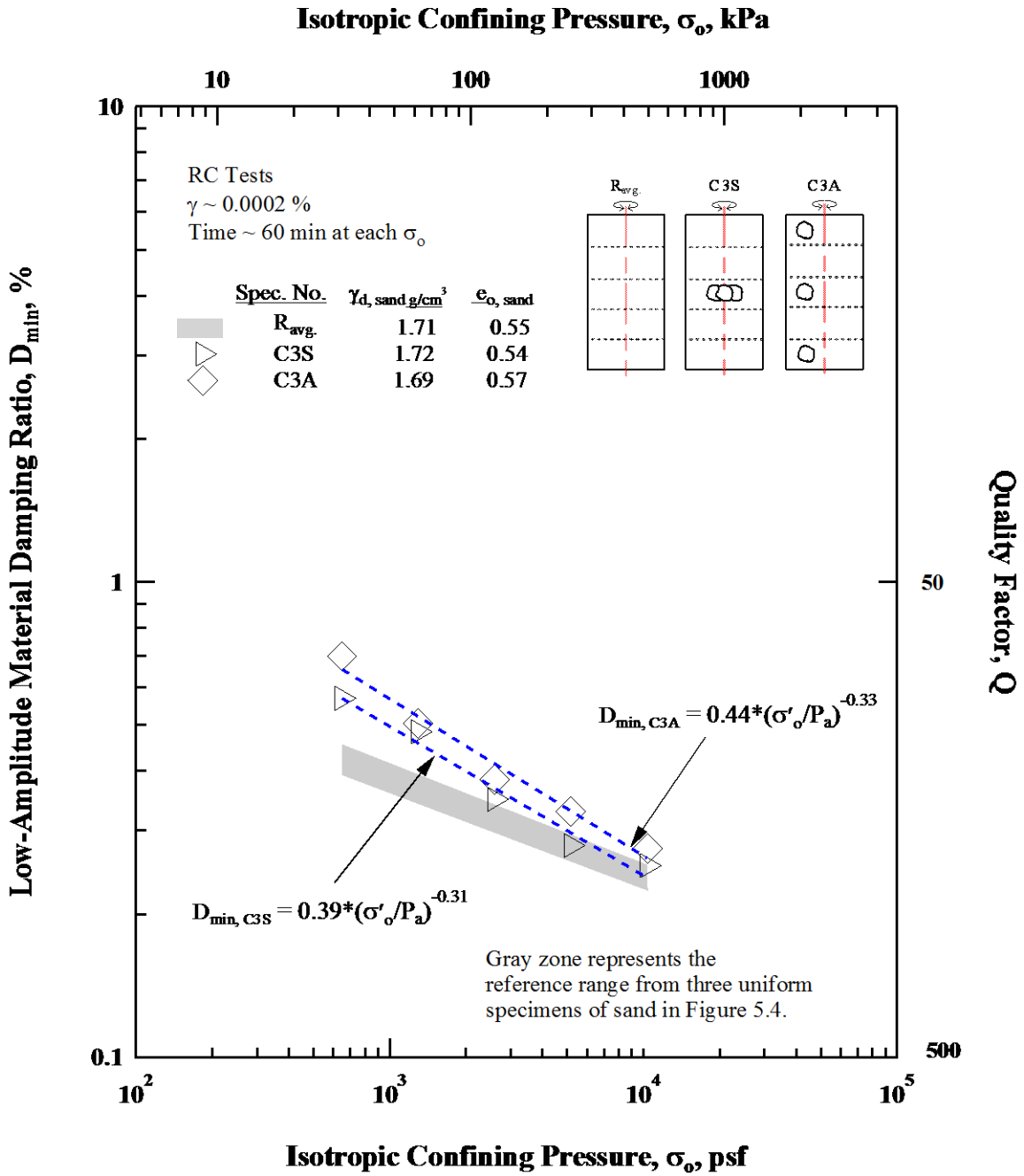


Figure 5.11 Comparison of the Variations of Low-Amplitude Material Damping Ratio with Isotropic Confining Pressure from Resonant Column Tests of Specimens R_{avg.}, C3S, and C3A

change in confining pressure than both the symmetrical specimen and the uniform reference sand.

In summary, the “relatively larger” and “large” oversized particles increased the small-strain material damping ratio (D_{\min}), even for symmetrical Specimen C4S. Additionally, Specimen C4A (containing offset gravel particles) showed higher energy dissipation than Specimen C4S, following the general trend shown in this work.

5.5 EFFECT OF MATERIAL TYPE

The effects on the dynamic properties of uniform gravel specimens constructed solely with the oversized particles were examined. 0.25-inches, 0.5-inches, and 0.8-inches gravel particles were constructed with Specimens C5, C6, and C7, respectively. Additionally, a heterogeneous material (a mixture of uniform sand and uniform gravel) was used to construct a special specimen, Specimen C8. In Specimen C8, the void in the uniform, 0.5-inches gravel were filled with the uniform washed mortar sand. This specimen was also tested.

The test results of Specimens G5 through G8 are shown in Figure 5.13 in terms of the $\log G_{\max} - \log \sigma_o$ relationship. The results for the three uniform sand specimens are presented as the gray zone in Figure 5.13 for comparison purposes. As seen, the three uniform gravel specimen as well as the sand-gravel mixture specimen showed higher small-strain shear modulus than the uniform sand. However, there was no major difference in the values of A_G for Specimens of C5 through C7. On the other hand, sand-gravel mixture, Specimen C8 showed not only a large increase in stiffness but also an increased sensitivity to confining pressure compared to the uniform gravel or the uniform sand specimens. The sand-gravel mixture had the highest with values of both A_G and n_G .

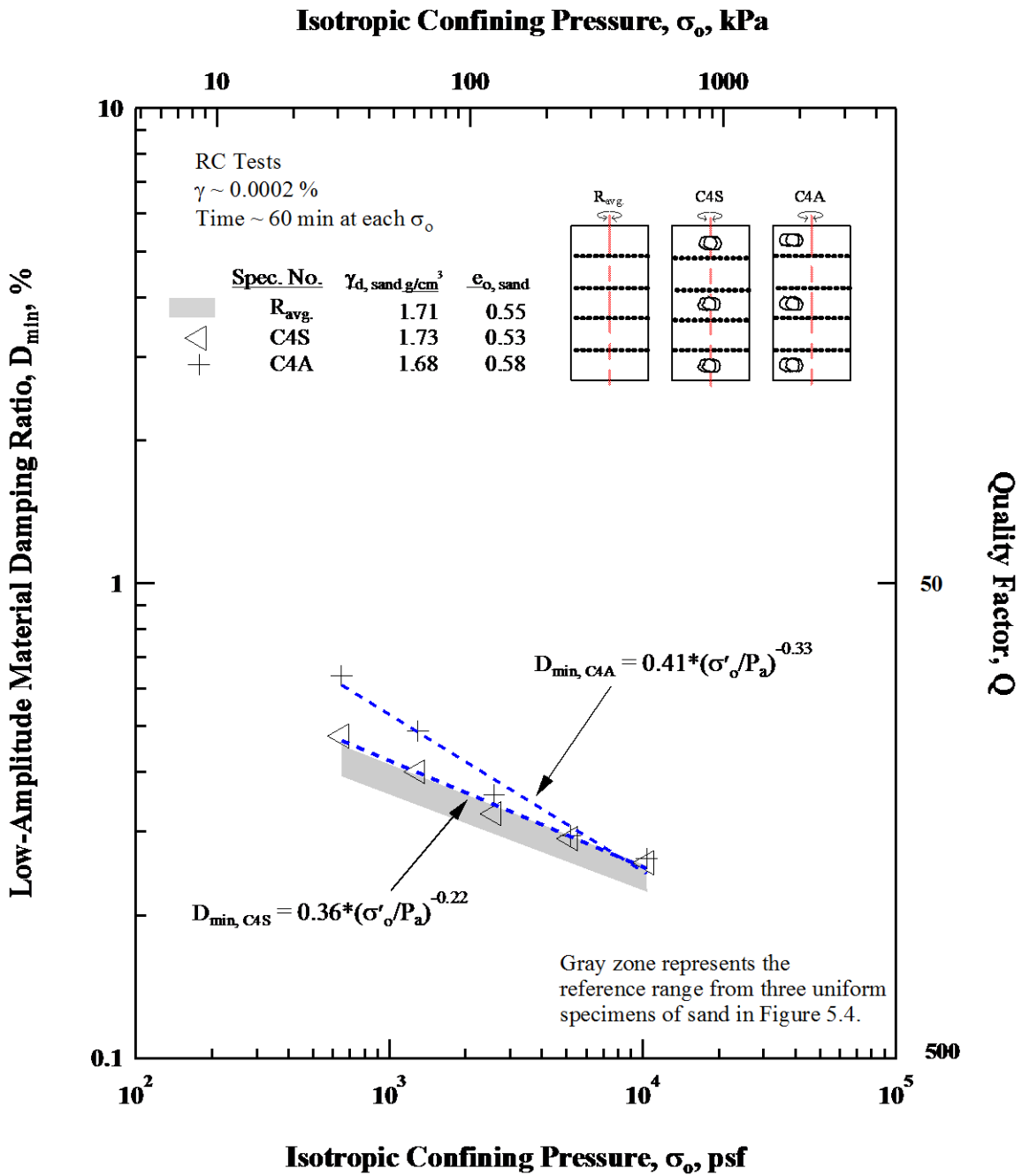


Figure 5.12 Comparison of the Variations of Low-Amplitude Material Damping Ratio with Isotropic Confining Pressure from Resonant Column Tests of Specimens R_{avg.}, C4S, and C4A

These differences are explained by the increase in C_u , implying that the material becomes more sensitive to changes in confinement as it becomes less uniform. These results agreed with Menq's (2003) tests that the sensitivity to confinement is only affected by C_u which, in this case, ranged from 1.14 to 1.46 for Specimens C5, C6, and C7.

The variation of material damping ratio with isotropic confining pressure for the uniform gravel specimens are compared with the sand-gravel mixture in Figure 5.14. Unlike the comparison of the $\log G_{\max} - \log \sigma_o$ relationships, there is no clear difference between the $\log G_{\max} - \log \sigma_o$ relationships. A further study for more comprehensive explanations about this difference is needed.

5.6 SUMMARY

Small-strain measurements were performed with the RCTS device on uniform sand specimens with and without gravel particles. For comparison purposes, uniform gravel specimens and a sand-gravel specimen were also tested. The effects of oversized particles on the dynamic properties in the small-strain range were first presented. As long as the oversized particles were near the axis of rotation, the particles had little effect on the dynamic properties (G_{\max} and D_{\min}) regardless of sizes and numbers of particles. However, once the oversized particles were located away from the axis of rotation and closer to the perimeter of the specimen, the oversized particles influenced the dynamic properties. In other words, the oversized particles located outside of the axis of rotation of the specimens increased both the shear modulus and material damping ratio. Finally, the effects of median grain size and uniformity coefficient on the small-strain dynamic properties were investigated using uniform gravel specimens and a sand-gravel specimen. The test results showed that the effect of a large uniformity coefficient, which represented

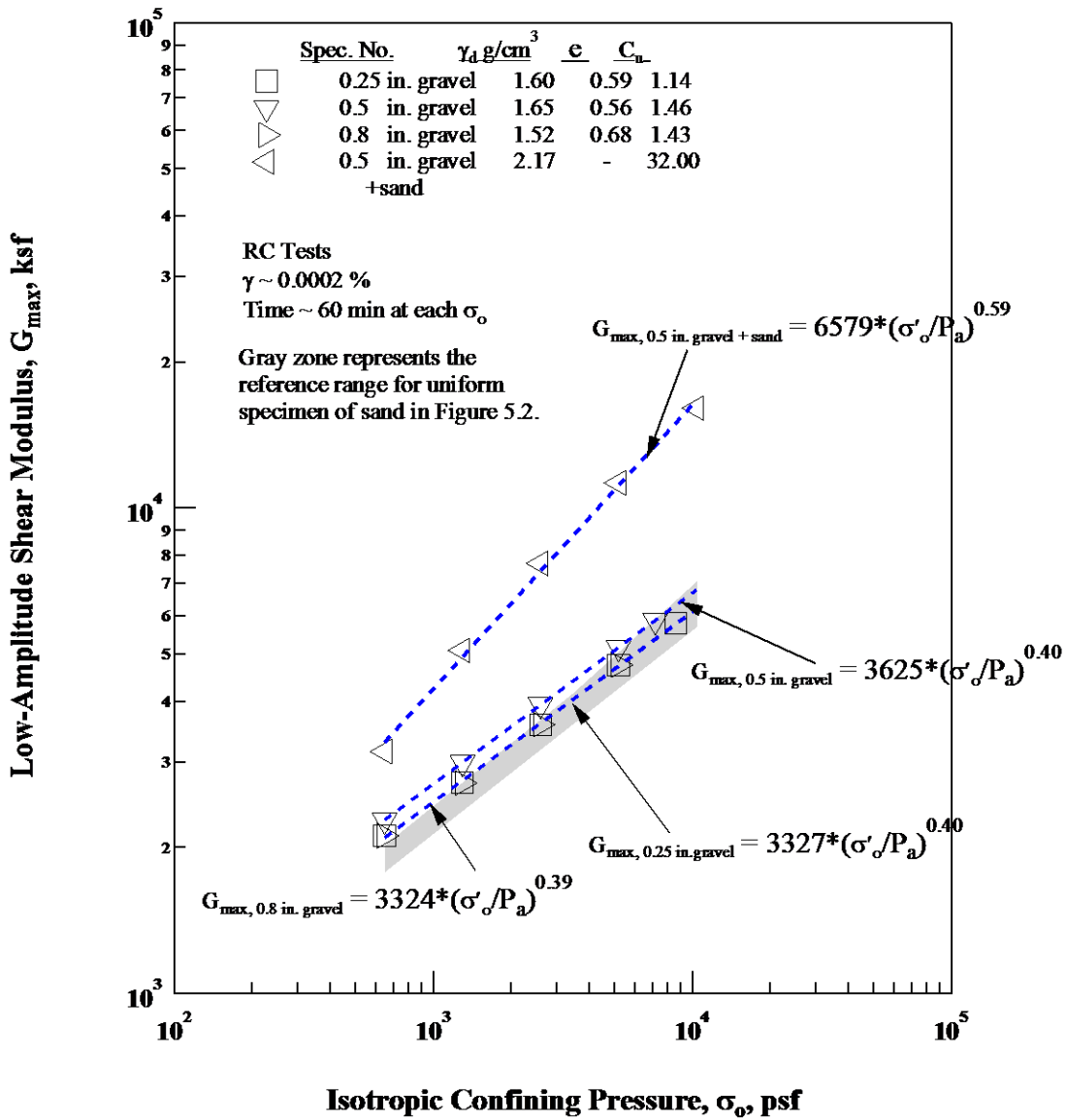


Figure 5.13 Comparison of the Variation of Low-Amplitude Shear Modulus with Isotropic Confining Pressure from Resonant Column Tests of Uniform Gravel Specimens (C5 through C8)

the sand-gravel mixture, had a significant effect on G_{\max} . No strong effect of median grain size was found in these tests.

CHAPTER SIX

EFFECT OF OVERSIZED PARTICLES ON NONLINEAR DYNAMIC PROPERTIES

6.1 INTRODUCTION

Shear modulus (G) in the nonlinear shear strain range and effects of oversized particles on shear moduli of uniform sand are discussed in Section 6.2. Material damping ratios in the nonlinear shear strain range of material damping ratio and the effects of the oversized particles on material damping ratios of uniform sand are discussed in Section 6.3. Finally, a summary of the effects of oversized particles of nonlinear G and D is summarized in Section 6.4.

6.2 NONLINEAR SHEAR MODULUS

High-Amplitude tests using the RCTS device were performed to examine the effects of oversized particles on the dynamic properties (G and D) in the nonlinear strain range. These tests were performed at confining pressures of 18 psi and 72 psi for Cases C1 to C4. Comparisons of the variation of shear modulus with shear strain at σ_o equal to 18 psi at 72 psi are presented in Figures 6.1 and 6.2, respectively. Reference ranges from the $G - \log \gamma$ relationships of the three uniform sand specimens at both pressures are presented as gray zones in the figures. It is clearly seen that the asymmetrically located oversized particles (C1A through C4A) have higher shear moduli at given strains than the specimens with symmetrically located oversized particles (C1S through C4S). A

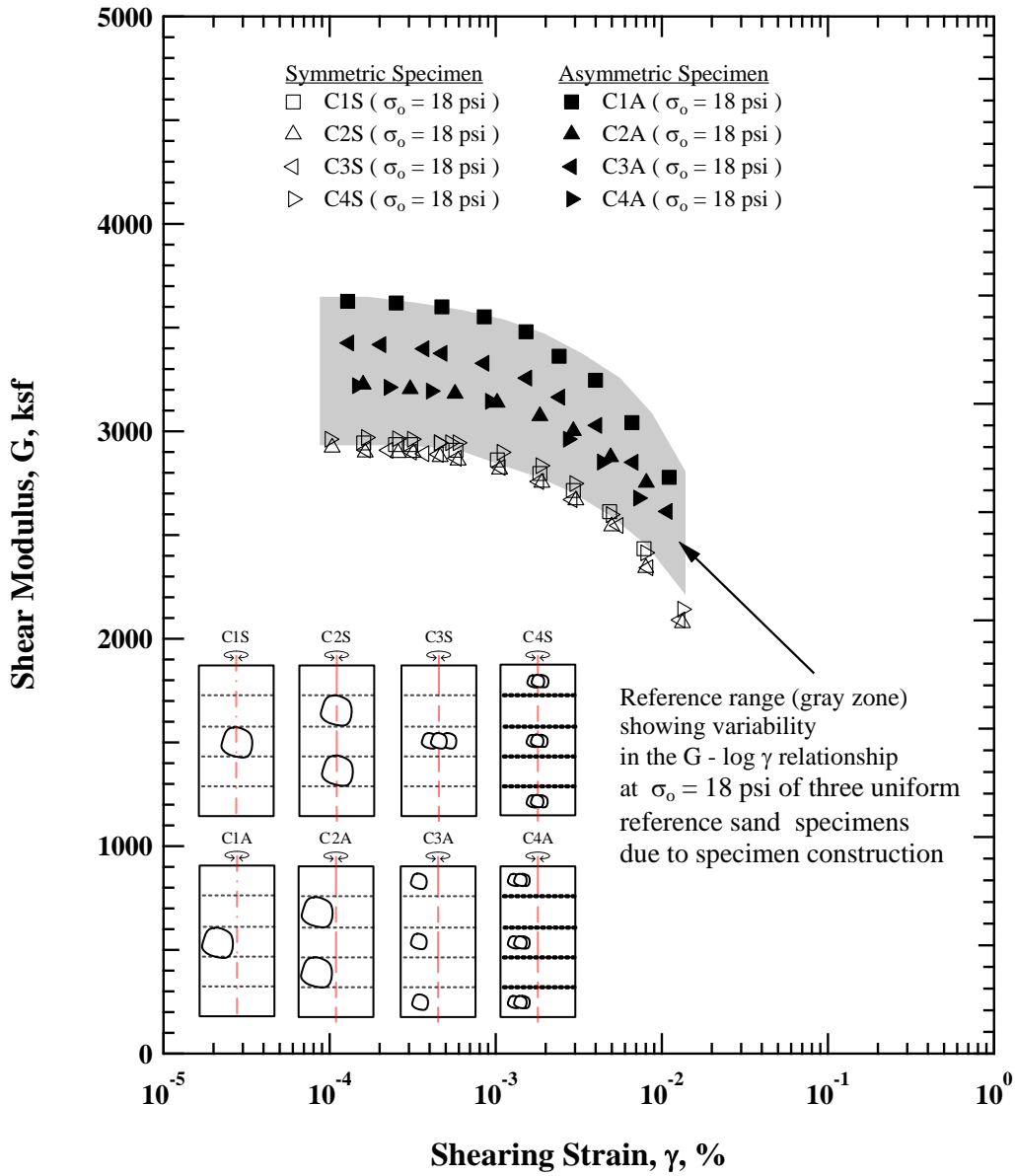


Figure 6.1 Variation in Shear Modulus with Shear Strain at an Isotropic Confining Pressure of 18 psi from Resonant Column Tests of C1 through C4 and the Uniform Reference Sand Specimens

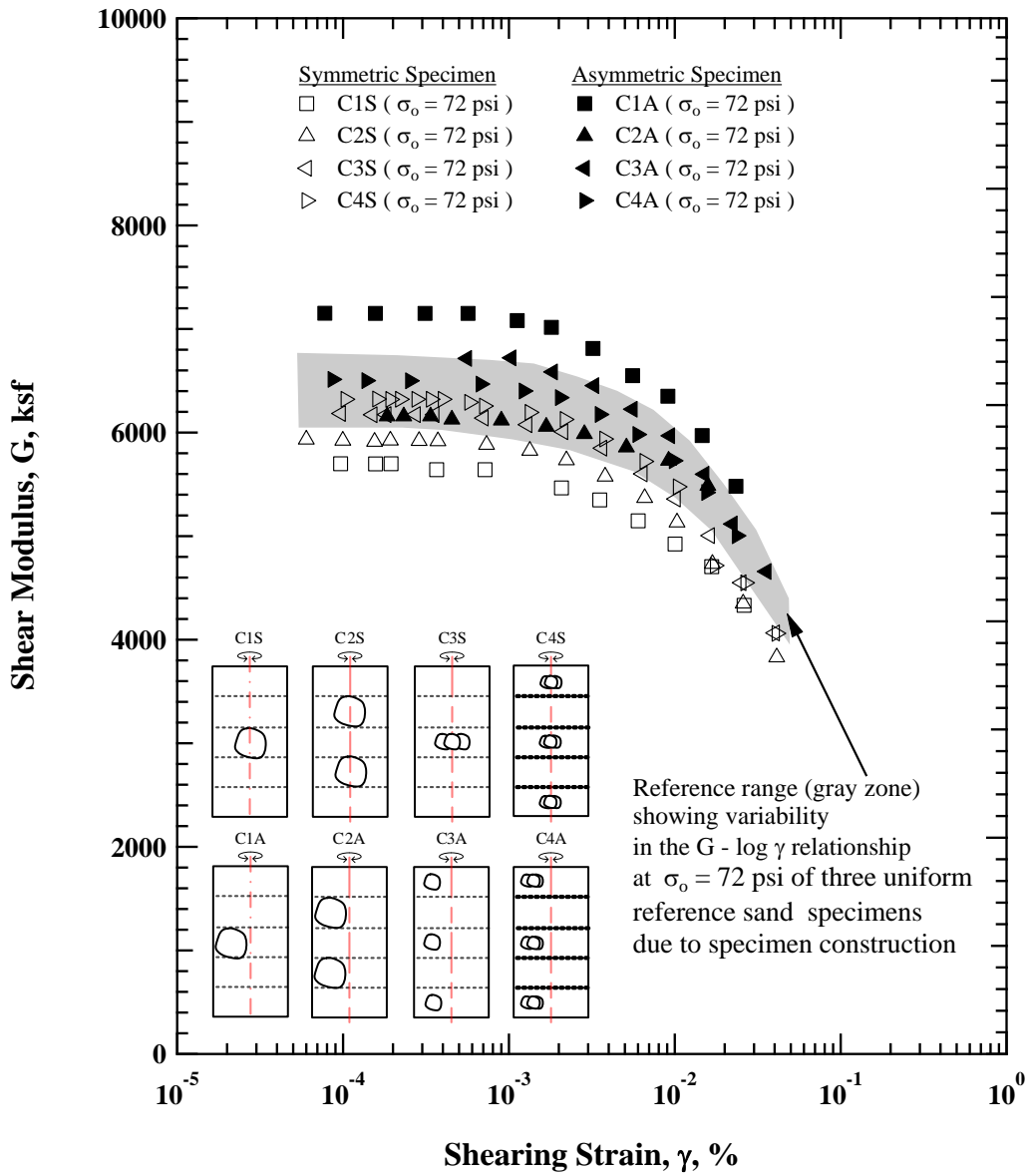


Figure 6.2 Variation in Shear Modulus with Shear Strain at an Isotropic Confining Pressure of 72 psi from Resonant Column Tests of C1 through C4 and the Uniform Reference Sand Specimens

noteworthy point is the similarity of the $G - \log \gamma$ curves for Specimens C1S through C4S at 18 psi (see Figure 6.1.) This similarity indicates that all cases of oversized particles located along the axis of rotation affect the values of G and their variation in the nonlinear strain range are nearly the same. Furthermore, the asymmetrical situations essentially make all cases of sand with oversized particles slightly stiffer than the uniform sand. In Figure 6.2, the $G - \log \gamma$ curves of Specimens C1S through C4S at 72 psi are somewhat more scattered than those at 18 psi, but this variability does not seem to be significant and the general trend are the same.

In Figures 6.3 and 6.4, the normalized shear modulus reduction curves for cases C1 through C4 at confining pressures of 18 psi at 72 psi are presented, respectively. An average curve of the $G - \log \gamma$ relationships for the three uniform sand specimens was also presented. As seen, there is essentially no significant difference in the normalized the $G/G_{\max} - \log \gamma$ relationships between all specimens, with the exception of that Specimen C2A behaved more linearly than the other specimens at both pressure levels. This difference might occurred because of the high density of Specimen C2A (see Table 4.3(a), in which Specimen C2A has the lowest initial void ratio, about 0.5).

6.3 NONLINEAR MATERIAL DAMPING RATIO

Dynamic measurements of material damping ratio in the nonlinear shear strain range were also performed during the RC-HAT tests. The variation of material damping ratio (D) with shear strain at confining pressures of 18 psi and 72 psi for cases C1 through C4 and the uniform sand specimens are present in Figures 6.5 and 6.6, respectively. As shown in the $G/G_{\max} - \log \gamma$ relationship, the $D - \log \gamma$ relationships are

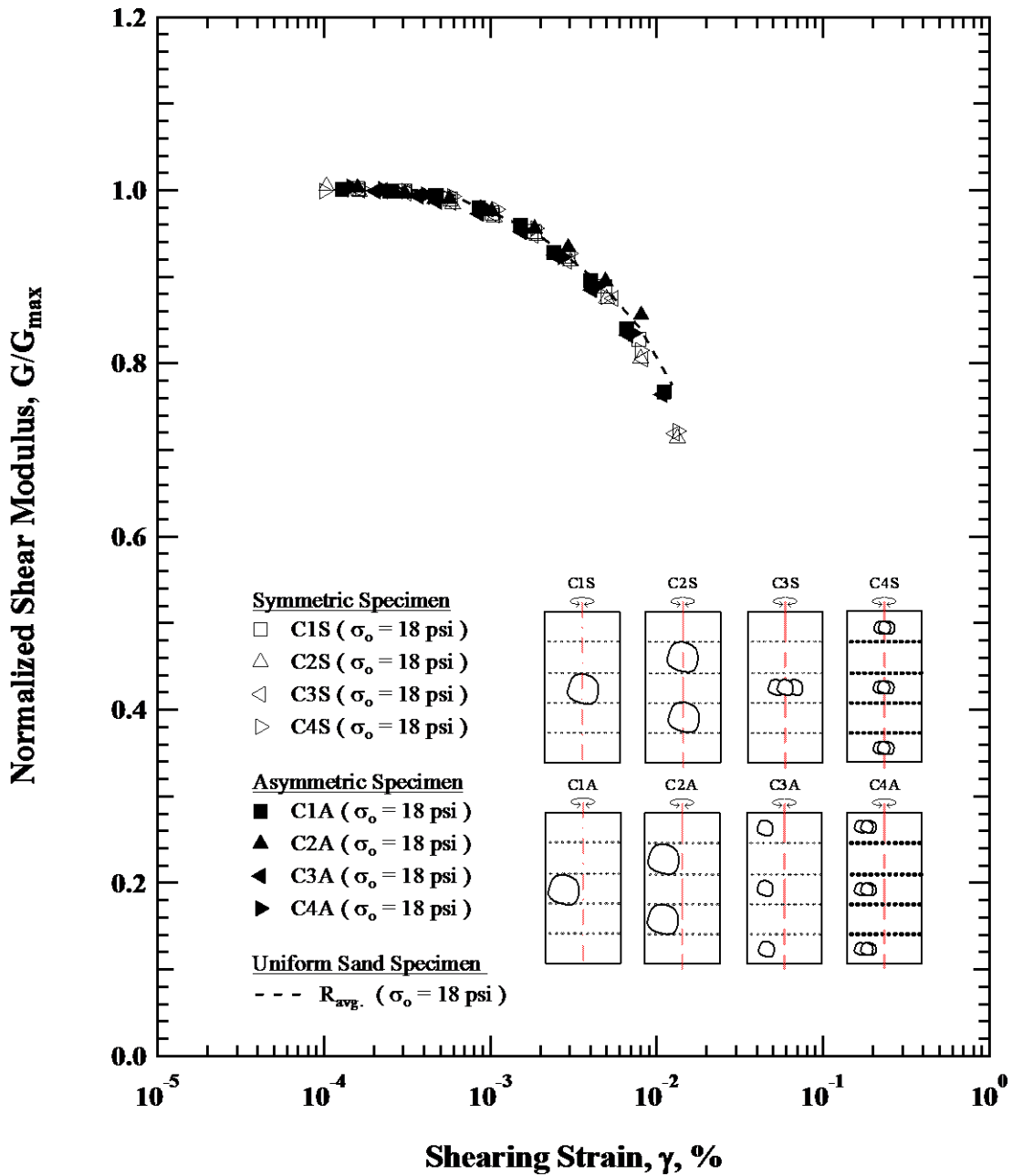


Figure 6.3 Variation in Normalized Shear Modulus with Shear Strain at an Isotropic Confining Pressure of 18 psi from Resonant Column Tests of Specimens C1 through C4 and the Uniform Reference Sand Specimens

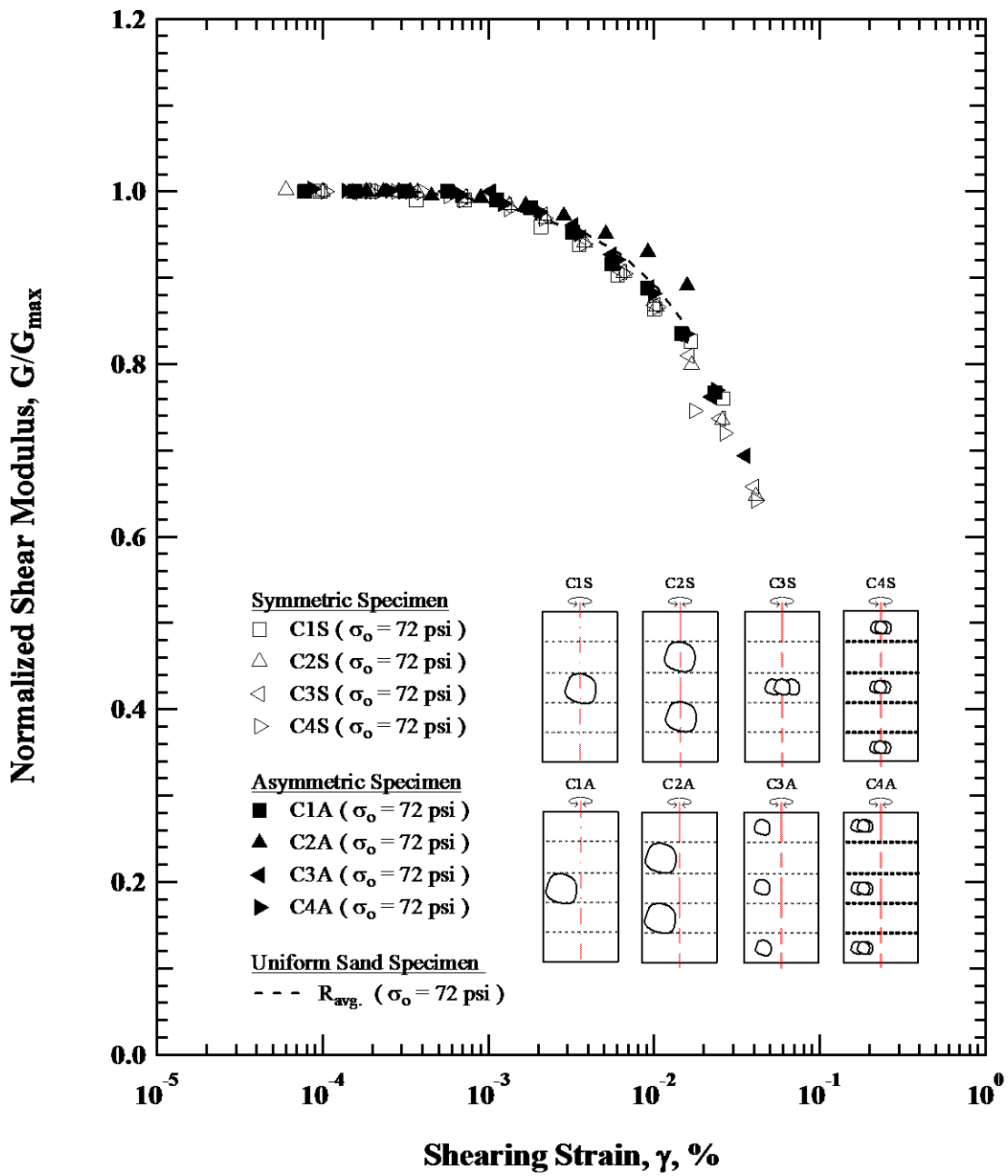


Figure 6.4 Variation in Normalized Shear Modulus with Shear Strain at an Isotropic Confining Pressure of 72 psi from Resonant Column Tests of Specimens C1 through C4 and the Uniform Reference Sand Specimens

nearly the same. The likely reason that the $D - \log \gamma$ relationships do not show a spread like the $G - \log \gamma$ relationships is that, over the strain range tested, G changes by less than 50% while D changes by about a factor of 20. This large change in D cancels any small effects created by the oversized particles in both figures. Specimen C2A behaved more linearly compared to the other specimens. As with the $G/G_{\max} - \log \gamma$ relationship, this increase of linearity was likely caused by the high density of Specimen C2A. From an overall point of view, the test results demonstrate that the sizes, numbers, and locations of oversized particles have a small effect on the material damping ratio.

6.4 SUMMARY

Measurements of the nonlinear dynamic behavior of uniform sand with and without oversized particles were performed using the RCTS device. In the high-amplitude testing, the effects of the oversized particles in the nonlinear range were most clearly exhibited in the $G - \log \gamma$ relationships. Specimens containing asymmetrically located particles were generally stiffer than uniform sand which was also slightly stiffer than specimens with symmetrically located particles. The $G/G_{\max} - \log \gamma$ and $D - \log \gamma$ relationships for the specimens were also determined in the RC tests. These comparisons showed that the additions of oversized particles located both symmetrically and asymmetrically in the uniform sand specimens have little impact on the nonlinear dynamic properties ($G/G_{\max} - \log \gamma$ and $D - \log \gamma$ relationships) which compared well with uniform sand.

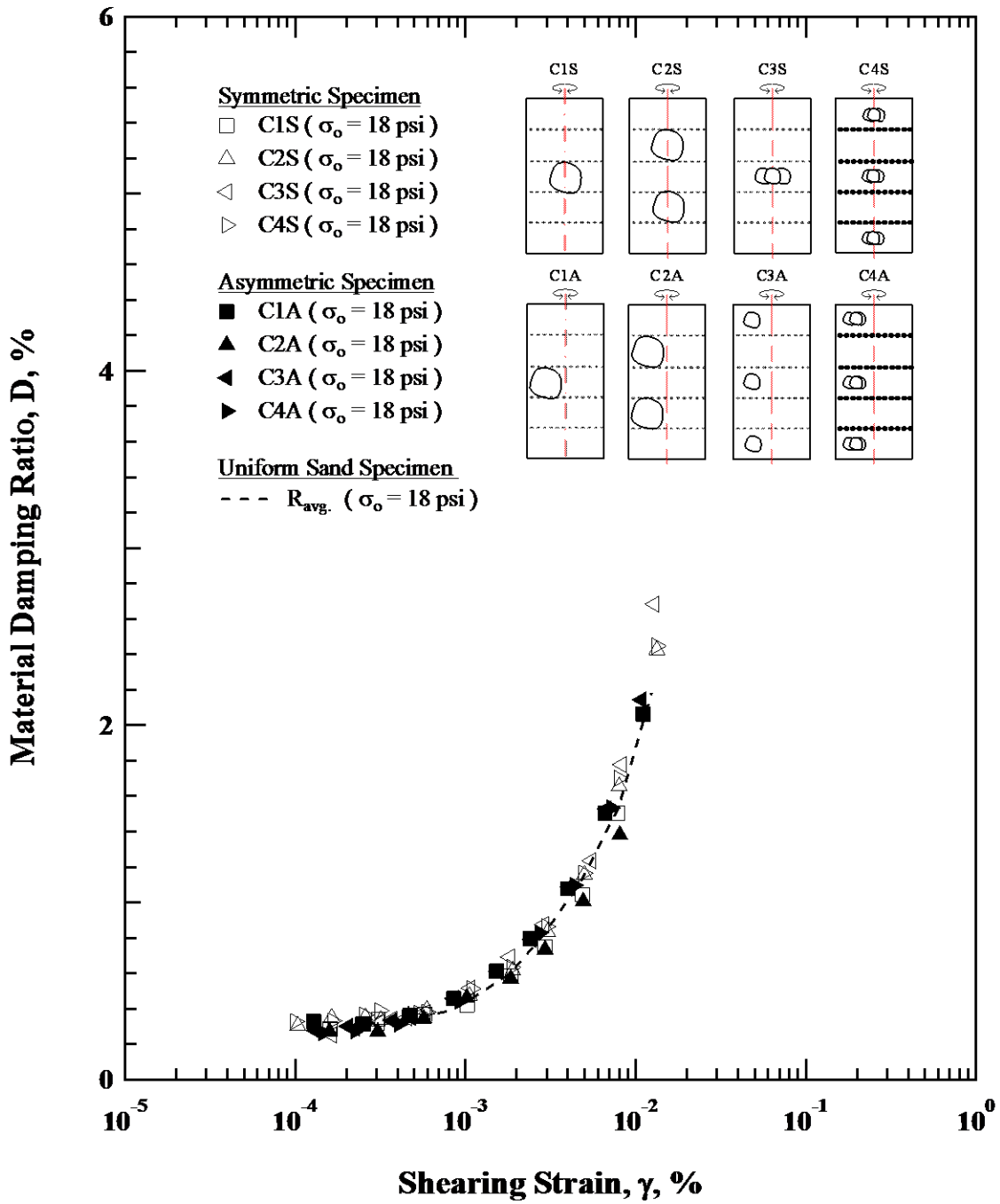


Figure 6.5 Variation in Material Damping Ratio with Shear Strain at Isotropic Confining Pressure of 18 psi from Resonant Column Tests of Specimens C1 through C4 and the Uniform Reference Sand Specimens

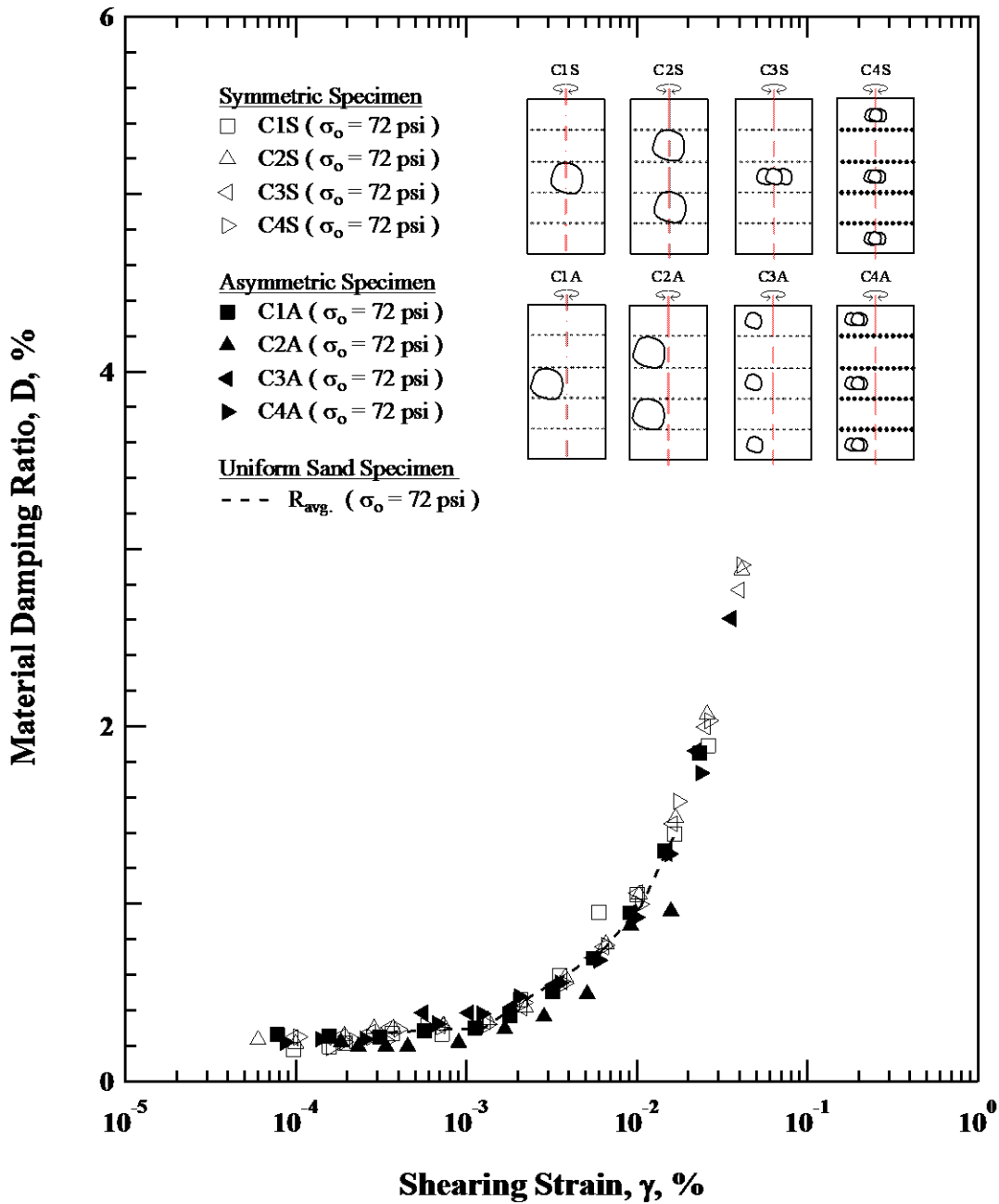


Figure 6.8 Variation in Material Damping Ratio with Shear Strain at Isotropic Confining Pressure of 72 psi from Resonant Column Tests of Specimens C1 through C4 and the Uniform Reference Sand Specimens

CHAPTER SEVEN

CONCLUSION

7.1 SUMMARY

In this thesis research, the effects of oversized particles on the dynamic properties of a reference uniform sand were investigated. The oversized particles were represented by gravel particles. The uniform sand was washed mortar sand from the Colorado River in Austin Texas. This sand was selected because material and dynamic properties are well known. This study was motivated by the fact that many times intact specimens with a number of oversized particles are dynamically tested in the laboratory with RCTS equipment. However, up to this time, the impact of the oversized particles on dynamic soil properties has been unknown. A total 14 of rounded gravel particles were selected for the oversized particles. The diameters of the gravel were greater than about 0.5 inches. This diameter is about one sixth of the 2.8 inches which was the selected diameter of all specimens constructed in this study. The gravel particles can be divided into three groups: (1) the “largest” particles, which were installed in specimens designated as Cases C1 and C2, (2) “relatively larger” particles, which were installed in specimens designated as Case C3, and finally (3) “large” particles, which were installed in specimens designated as Case C4. Cases C1 through C4 are each composed of two types specimens as follows: (1) ones with the gravel particles symmetrically located and (2) ones with the gravel particles and asymmetrically located. Fundamental physical investigations were performed on the oversized particles to characterize specific gravity, average diameters, weights and

volumes. Grain-size distribution curves were determined for all sand, sand-gravel and gravel specimens.

Three uniform sand specimens were first reconstituted and tested in the RCTS device. From the uniform sand test results, a reference range representing the variability due to specimen construction of the uniform sand was determined. Measurements of linear (small-strain) and nonlinear dynamic properties on the specimens were performed and analyzed.

7.2 CONCLUSIONS

7.2.1 Measurements in the Linear Strain Range

7.2.1.1 *Shear Modulus*

Dynamic measurements were performed on the uniform sand specimens with and without gravel particles. The variability due to construction of the uniform sand specimens in the $\log G_{\max} - \log \sigma_o$ relationships was small (less than $\pm 10\%$). This variability was used as a reference range that allowed the effects of oversized particles to be compared to the uniform sand specimens. In general terms, effects on G_{\max} of oversized particles in uniform reference sand were easily measured but were not large. However, one important finding from Cases C1 and C2 is that the “largest” oversized particles located asymmetrically, meaning particles with offset from the central section of the specimen, made the specimen slightly stiffer than the symmetrical case with the particles along the outer line of the specimen. This result indicates the location of oversized particles does affect the shearing stiffness of the basically sand specimen. This increase in G_{\max} was also readily recognized in the Case C3 specimens. On the other hand, the effect of the “large” particles located symmetrically or asymmetrically in the Case C4 specimens was not much different. These

results indicate that the size, number and location of oversized particles can affect the measured G_{\max} values. The effect can be an increase or decrease but the effect seems to be less than 15 %.

7.2.1.2 Material Damping Ratio

The measurements of small-strain material damping ratio (D_{\min}) were performed on the sand specimens with and without gravel particles. The variability due to specimen construction from the three uniform sand specimens in terms of the $\log D_{\min} - \log \sigma_o$ relationships was also used as a reference range and compared to the cases of sand with gravel particles. An increase of D_{\min} values occurred when the “largest” particles (G1 or G2 or their combination) were located away from the longitudinal axis of rotation in the specimens, hence asymmetrically located. This effect likely results from the situation that the particles offset from the axis of rotation fall in the region where the strain in the torsionally loaded specimens is larger and the oversized particles behaves like local intensifier of strain, even if the average strain level that the specimen is experiencing is small. As a result, the oversized particles located along the central, longitudinal axis of rotation, where the smallest strain occurs, have little effect on increasing material the damping.

The symmetrical specimens in Case C3 with the “relatively larger” oversized particles exhibited higher D_{\min} values than the uniform reference sand and the symmetrical Specimens C1S and C2S. The relative increases likely occurred because not only was the equivalent diameter of gavel particles G3, G4 and G5 larger compared to the “largest” particles (G1 or G2), but also because the increase of contact area allows more energy

dissipation in the specimens. The increase of contact area between particles also affected the increase of D_{\min} values in symmetrical Specimen C4S with symmetrically located particles. The increases in material damping due to the asymmetrical locations of the “relatively larger” and “large” oversized particles in the small-strain range were also found in Specimens C3A and C4A, respectively.

These results imply that the measurements of material damping ratio are more sensitive to the locations of oversized particles than the shear modulus measurements in the small-strain range. In addition, the increase of D_{\min} values due to the location of oversized particles deserves study and experiments in the future.

7.2.1.3 Effect of Material Type

The effects of granular material type, expressed by uniformity coefficient, C_u , on the dynamic properties was also investigated in the small-strain range. This investigation involved uniform gravel specimens, a mixed sand-gravel specimen, and the uniform sand specimens. Specimen C8 (the sand-gravel mixture) showed higher stiffness and increased sensitivity to confining pressure due to the high value of C_u (uniformity coefficient) relative to the other specimens. On the other hand, the effect of median grain size, D_{50} , was not clear in this comparison study. Finally, a strong correlation between material damping ratio in small-strain range and the grain distribution characteristics (C_u and D_{50}) was not found in this study.

7.2.2 Measurements in the Nonlinear Strain Range

High-amplitude resonant column tests were performed to study the nonlinear behavior of uniform sand specimens with and without oversized particles. The variation of shear modulus with shear strain ($G - \log \gamma$) was obtained in these tests. Increases in the $G - \log \gamma$ relationships in the nonlinear strain range when the oversized particles were located away from the axis of rotation (asymmetrical location) were found. On the other hand, small decreases in the $G - \log \gamma$ relationships were found when the oversized particles were symmetrically located. However, differences in the $G - \log \gamma$ relationships between specimens containing the oversized particles and uniform sand were rather small ($< 10\%$). In addition, the characteristics of oversized particles such as sizes, numbers and locations affected the $G/G_{\max} - \log \gamma$ and $D - \log \gamma$ curves very little.

7.3 RECOMMENDATIONS

1. The relationship between the change of G_{\max} and D_{\min} due to the asymmetrical location of oversized particles in test specimens and local strain variations around the specimen perimeter is worthy of further investigation. This study could also be strongly supported by a particulate mechanics study.
2. The development of a parameter or parameters to quantify the effects of oversized particles on nonlinear dynamic properties is also needed. The $G - \log \gamma$ relationships, in particular, need further study. Parameters which can be applied to intact soil specimens to estimate variability and

uncertainty would be helpful in obtaining practical engineering solutions.

3. Examination of the effects of oversized particles on the dynamic properties in field would also be helpful in providing a better understanding of this phenomenon. Field testing should incorporate scaling based on wavelengths involved in the measurement.

REFERENCES

- ASTM D 2487-00 (2000). "Standard Classification of Soils for Engineering Purposes (Unified Soil Classification System)." pp. 1-11.
- ASTM D 4015-07. (2007), "Standard Test Methods for Modulus and Damping of Soils by the Resonant-Column Method."
- Bolt, B.A. (1976), "Nuclear Explosions and Earthquakes", W.H. Freeman and Company.
- Darendeli, B. M. (2001), "Development of a new family of normalized modulus reduction and material damping curves." *Ph. D. Dissertation*, The University of Texas at Austin., 362 p.
- Hall, J.R., Jr. and Richart F.E., Jr. (1963). "Effects of Vibration Amplitude on Wave Velocities in Granular Materials," *Proceedings*, Second Pan-American Conference on Soil Mechanics and Foundations Engineering, Vol. 1, pp. 145-162.
- Hardin, B. O. and Black, W. L. (1968). "Vibration Modulus of Normally Consolidated Clay." *J. of Soil Mech. and Found. Div.*, ASCE, Vol. 94 No. SM2, pp 353-369.
- Hardin, B. O. and Drnevich, V. P. (1972), "Shear Modulus and Damping in Soils: Measurement and Parameter Effects." *J. of Soil Mech. and Found. Div.* ASCE, Vol. 98 No. SM6, pp. 603-624.
- Hardin, B. O. (1978). "The nature of stress-strain behavior of soils." *Proceedings*, Geotech. Eng. Div. Specialty Conf. on Earthquake Eng. and Soil Dynamics, Vol. 1 ASCE, Pasadena, pp. 3-90.
- Hwang, S. K. (1997). "Investigation of the Dynamic Properties of Natural Soils," *Ph.D. Dissertation*, University of Texas at Austin, 394 pp.
- Isenhower, W.M. (1979). "Torsional Simple Shear / Resonant Column Properties of San Francisco Bay Mud," *M.S. Thesis*, University of Texas at Austin, 307 pp.
- Ishihara, Kenji. (1996), *Soil Behaviour in Earthquake Geotechnics*. J.M. Brady, C.E. Brennen, W.R. Eatock Taylor, M.Y. Hussaini, T.V. Jones, and J. Van Bladel, Eds.
- Kim, D.S. (1991), "Deformational Characteristics of Soils at Small to Intermediate Strains from Cyclic Tests." *Ph.D. Dissertation*, The University of Texas at Austin, 341 p.
- Kokusho, T. (1980), "Cyclic Triaxial Test of Dynamic Soil Properties for Wide Strain Range" *Soils and Foundations*, 20, pp. 45-60.

- Kokusho, T. (1987) "In Situ Dynamic Soil Properties and Their Evaluation." *Proceeding of the 8th Asian Regional Conference on Soil Mechanics and Foundation Engineering*, Kyoto, Vol. 2, pp.215-435.
- Krama, S.L. (1996), *Geotechnical Earthquake Engineering*, Prentice Hall, Upper Saddle River, N.J., pp. 19, 551.
- Laird, J. P. (1994). "Linear and Nonlinear Dynamic Properties of Soil at High Confining Pressures," M.S. Thesis, University of Texas at Austin, 291 p.
- Lodde, P.F. (1982). "Shear Moduli and Material Damping of San Francisco Bay Mud," *M.S. Thesis*, University of Texas at Austin.
- Masing, G. (1926) "Eigenspannungen und Verfestigung Beim Masing," *Proceedings*, Second International Congress of Applied Mechanics, pp.332-335.
- Menq, F.-Y. (2003), "Dynamic Properties of Sandy and Gravelly Soils." *Ph.D. Dissertation*. University of Texas at Austin. 364 p.
- Ni, S.-H. (1987), "Dynamic Properties of Sand Under True Triaxial Stress States from Resonant Column/Torsional Shear Tests." *Ph.D. Dissertation*, The University of Texas at Austin, 421 pp.
- Richart, J. E., Jr., Hall, J. R., Jr. and Woods R. O. (1970) *Vibrations of Soils and Foundations*, Prentice-Hall Inc. Englewood Cliff, New Jersey, 414 p.
- Seed, H. B., Wong, R. T., Idriss, I. M. and Tokimatsu, K. (1986), "Moduli and Damping factors for Dynamic Analyses of Cohesionless Soil." *J. of Geotech. Engr.*, ASCE, Vol. 112, No. GT11, pp. 1016- 103.
- Tanaka, Y., Kudo, K., Nishi, K., and Okamoto, T. (1994). "Shear modulus and damping ratio of gravelly soils measured by several methods." *Pre-Failure Deformation of Geomaterials, Vol I*. Mitachi & Miura, Eds. pp 47-53.
- Song, C.R. (1986), "Effects of Gradation and Cycles of Loading on Dynamic Properties of Silty Sands." *M.S. Thesis*, The University of Texas at Austin.
- Stokoe, K. H., II, Wright, S. G., Bay, J. A. and J. M. Roesset, (1994), "Characterization of Geotechnical Sites by SASW Method," ISSMFE Technical Committee 10 for XIII ICSMFE, Geophysical Characteristics of Sites, A.A. Balkema Publishers/Rotterdam & Brookfield, Netherlands, pp. 785-816.
- Stokoe, K. H., II, Darendeli, M. B., Andrus, R. D. and Brown, L. T. (1999). "Dynamic soil properties: laboratory, field and correction studies." Seco e Pinto, (ed.), *Proceedings, Second Int. Conf. On Earthquake Geotechnical Engineering*, Lisbon. 21-25 June 1999, (3): pp. 811-845, Rotterdam, Balkema.

Stokoe, K.H. (2011). *Soil and Rock Dynamics*. The University of Texas at Austin. Spring 2011. Course Notes and Presentation.

Van Hoff, D.J. (1993). "Evaluation of the Dynamic Properties of Artificially Cemented Sand at Low Confining Pressures", Ph.D. Dissertation, Geotechnical Engineering, Department of Civil Engineering, University of Texas at Austin, May.

VITA

Boonam Shin was born in Seoul, South Korea in August, 1983. He was the second child of Yong Shin and Ducklim Lee and has one older sister, May Shin. After graduating from Sanggye High School in 2002, he attended the Sungkyunkwan University in South Korea where he studied Civil and Environmental Engineering. He graduated from SKKU with a B.E. degree in May 2011 and entered the graduate school at the University of Texas at Austin in August 2011.

Email address: bnshin83@gmail.com

This thesis was typed by the author.